

Synthesis, Spectroscopic and Nonlinear Optical Properties of Multiple [60]Fullerene–Oligo(*p*-phenylene ethynylene) Hybrids

Yuming Zhao,^[a] Yasuhiro Shirai,^[b] Aaron D. Slepko,^[c] Long Cheng,^[b] Lawrence B. Alemany,^[b] Takashi Sasaki,^[b] Frank A. Hegmann,^{*,[c]} and James M. Tour^{*,[b]}

Abstract: A series of multiple [60]fullerene terminated oligo(*p*-phenylene ethynylene) (OPE) hybrid compounds has been synthesized through a newly developed in situ ethynylation method. Structural and magnetic shielding properties of the highly unsaturated carbon-rich C₆₀ and OPE scaffolds were characterized by 1D and 2D NMR spectroscopic analyses. Electronic interactions between the [60]fullerenes and the OPE backbones were investigated by UV/Vis spectroscopic and cyclic voltammetry (CV) experiments. Our studies clearly show that although the multiple [60]fullerene

groups are connected via π -conjugated OPE frameworks, they present diminutive electronic interactions in the ground state, and the electronic behavior of the [60]fullerene cages are only affected by the OPE backbones through modest inductive effects. Interestingly, sizable third-order nonlinear optical (NLO) responses (γ) and enhanced two-photon absorption (TPA) cross-sections ($\sigma^{(2)}$) were determined


for the multifullerene–OPE hybrid **31** relative to its OPE precursor from differential optical Kerr effect (DOKE) experiments. Such enhanced NLO performance is presumably due to the occurrence of periconjugation and/or charge transfer effects in the excited state. In addition, comparatively strong excited-state absorption was observed and characterized for OPE pentamer **12**. Thus, the use of such fullerene-derivatized conjugated oligomers aids the quest for molecules with large third-order NLO and TPA properties.

Keywords: conjugation • electrochemistry • fullerenes • NMR spectroscopy • nonlinear optics

Introduction

There is an active search for novel conjugated organic materials capable of functioning as key components in a wide range of electronic and photonic devices.^[1–3] Toward this end, a myriad of π -conjugated systems have been synthesized and investigated in the past two decades. Extensive research attention has been focused on π -conjugated oligomer/polymer systems such as oligo(enyne)s,^[4,5] polyynes,^[6] oligo(arylene ethynylene)s,^[7] oligo(arylene vinylene)s,^[8,9] and oligo(thiophene)s,^[10–12] owing to their diverse and tunable electronic and photonic properties, as well as the flexibility and ease with which these organic materials are handled. Such research has considerably widened the applicability of organic-based materials with respect to the fields of molecular electronics,^[13,14] opto-electronics,^[15,16] and organic nonlinear optics,^[17–19] to name but a few. The derivatization of conjugated oligomers with various electro- and photo-active functional groups has emerged as an important approach to the design and discovery of useful materials for molecular electronic and photonic devices. In particular, molecules with highly delocalized and polarizable π -electron density

- [a] Prof. Dr. Y. Zhao
Department of Chemistry
Center for Nanoscale Science and Technology
Rice University, MS-222, 6100 Main St.
Houston, TX 77005 (USA)
Current address:
Department of Chemistry, Memorial University of Newfoundland
St. John's, Newfoundland, A1B 3X7 (Canada)
- [b] Y. Shirai, Dr. L. Cheng, Dr. L. B. Alemany, T. Sasaki,
Prof. Dr. J. M. Tour
Department of Chemistry
Center for Nanoscale Science and Technology
Rice University, MS-222, 6100 Main St.
Houston, TX 77005 (USA)
Fax: (+1) 713-348-6250
E-mail: tour@rice.edu
- [c] A. D. Slepko, Prof. Dr. F. A. Hegmann
Department of Physics, University of Alberta
Edmonton, AB T6G 2J1 (Canada)
Fax: (+1) 780-492-0714
E-mail: hegmanna@phys.ualberta.ca

 Supporting information for this article is available on the WWW under <http://www.chemeurj.org/> or from the author.

are among the most intensively studied species for such purposes.

Of great interest is the Buckminster [60]fullerene—an appealing carbon allotrope with an aesthetic football-shaped molecular structure, unique three-dimensional π -electron delocalization pattern, and small dimensions (ca. 0.7 nm in diameter).^[20,21] Since its discovery in the late 1980s, [60]fullerene (henceforth denoted *fullerene*) and its derivatives have been found to exhibit many extraordinary electronic and photonic properties, such as the unique electrochemical and optical absorption features in the excited state.^[22,23] Accordingly, fullerenes provide a useful platform for the design of new materials in the fields of artificial photosynthetic mimics,^[24] long-range intramolecular energy/charge transfer,^[25,26] efficient photon-energy conversion,^[27–29] photoinduced long-lived charge-separation species,^[30] optical devices based on second- and third-order nonlinear optical (NLO) behavior, multiple photon absorption processes,^[31–33] and optical limiters.^[34] However, the direct application of pristine fullerene in device fabrication has been limited by its poor solubility in most solvents, and in particular polar-organic solvents. Different approaches have been explored to overcome this obstacle, and much effort has been invested in blending fullerenes into various solid matrices of polymers and inorganic composites,^[35,36] as well as non-covalently encapsulating fullerene molecules into soluble host molecules such as [*n*]calixarenes^[37,38] and cyclodextrins.^[39] Covalent functionalization of fullerene,^[40,41] on the other hand, is attracting wide interest as it can greatly alter the physical and chemical properties of fullerene to readily achieve desired processabilities and performance. Clearly, new synthetic methodologies for fullerene derivatization are continuously important for synthetic organic chemists.

Our group is interested in integrating multiple fullerenes in various π -conjugated oligomers^[29] so as to develop new electronic and photonic properties. In principle, such hybridized fullerene–oligomer compounds would feature not only the intrinsic properties of individual fullerenes and conjugated oligomers, but in some circumstances new behavior and functions arising from the mutual interactions between fullerenes and oligomers.^[42] The synthesis of rigid conjugated oligomeric structures containing more than one fullerene moiety is a challenging task. Synthetically, the low solubility together with the moderate-to-low yields of multiple fullerene derivatives makes it extremely difficult to develop suitable reaction protocols. In addition, the isolation of products using conventional chromatographic means tends to be problematic for the same reasons. Currently there is a lack of reliable and facile synthetic methodologies for making the multiple-fullerene–oligomer compounds. Reported fullerene derivatization methods, including 1,3-dipolar and [4+2]-cycloaddition reactions, yield the fullerene derivatives primarily in the forms of fullerene-pyrollidines,^[43–48] methanofullerenes,^[49–55] and fullerene-acenes.^[56,57] Through these reactions, fullerenes and organic substituents are usually bonded to give irregular and distorted molecular shapes, with more than one sp^3 carbon between the fullerenes and

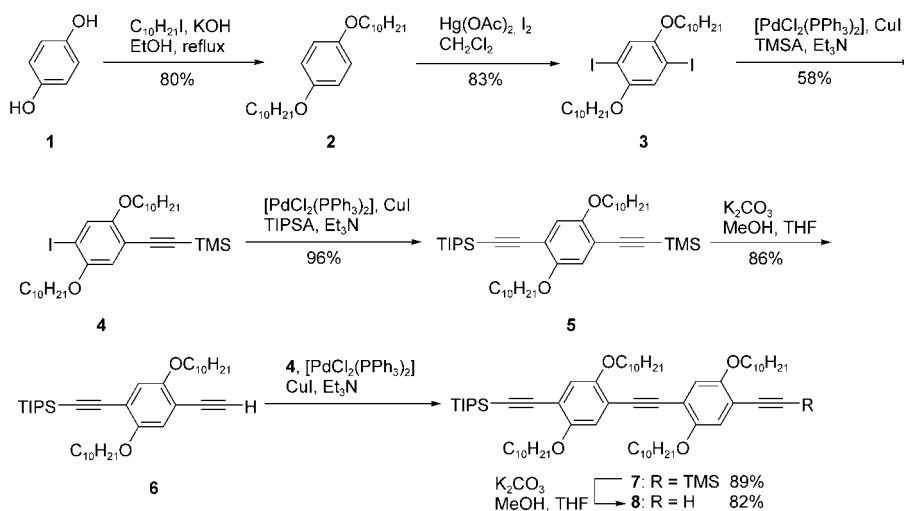
conjugated oligomers.^[58–65] As such, the molecules would likely show through-space rather than through-bond interactions between each electronically active unit. Although extensively used, these methods show limitations in terms of strengthening fullerene–oligomer interactions and forming regularly patterned molecular assemblies. Multiple-fullerene containing molecules synthesized by the ethynylation reaction,^[66–68] however, are rare and are far from being thoroughly addressed in the literature. Unlike other types of fullerene derivatives, the organic substituents are closely linked to the fullerene cages via an acetylenic bond in a nearly linear geometry, with only one sp^3 carbon bridging the conjugated path on the fullerene and its pendant groups. In this case, the fullerene π -electrons may possibly communicate with the alkynyl π -electrons in a through-space p-orbital overlapping mechanism, namely “periconjugation.”^[42,69–71] It is likely that such structural features would give rise to enhanced electronic interactions between fullerenes and conjugated functionalities, thereby providing a uniformly shaped molecular building block (tecton) for the construction of various molecular machinery and nano-architectures, as well as supramolecular assemblies.

In our previous work,^[72] we have described an efficient and facile synthesis of a series of multiple-fullerene terminated conjugated oligo(*p*-phenylene ethynylene)s (OPEs) via a novel in situ ethynylation methodology. Herein, along with complete synthetic details, we primarily highlight the electronic and optical characterization of these materials. First, we describe the synthesis of π -conjugated OPE molecules and their fullerene derivatives. Next, the structural and magnetic shielding properties of the multifullerene–OPE hybrids are elucidated with 1D and 2D NMR spectroscopic analyses. Then, the electronic absorption behavior and electrochemical redox properties characterized by UV/Vis spectroscopy and cyclic voltammetry (CV) are presented. Finally, we report on the molecular third-order hyperpolarizabilities (γ), two-photon absorption (TPA) cross section ($\sigma^{(2)}$), and excited-state absorption of selected OPE molecules **12**, **14** and fullerene–OPE hybrid **31** as studied with the differential optical Kerr effect (DOKE) technique.^[73]

Results and Discussion

Synthesis of OPE precursors: The synthesis of a series of linearly conjugated phenylene acetylene oligomers is outlined in Schemes 1 and 2. The essential building block **3** for the elongation of OPE chains was prepared via alkylation and iodination of 1,4-dihydroquinone (**1**). The incorporation of the decyloxy group is necessary to gain sufficient solubility for both the long-chain OPEs and their fullerene derivatives. In addition, the polar nature of the alkyloxy groups turns out to be very beneficial to subsequent column chromatographic separations. Next, monoiodide **4** was obtained from cross coupling 0.7 equiv of trimethylsilylacetylene (TMSA) with **3** under Sonogashira conditions. Compound **4** was then cross-coupled with triisopropylacetylene (TIPSA)

under palladium catalysis to yield unsymmetrically protected phenyl acetylene monomer **5**. Selective desilylation of the TMS group in the presence of K_2CO_3 gave **6**, which was converted to dimeric phenyl acetylenes **7** and **8** after another iteration of cross-coupling/desilylation.



Scheme 1. Synthesis of building blocks for long-chain OPEs.

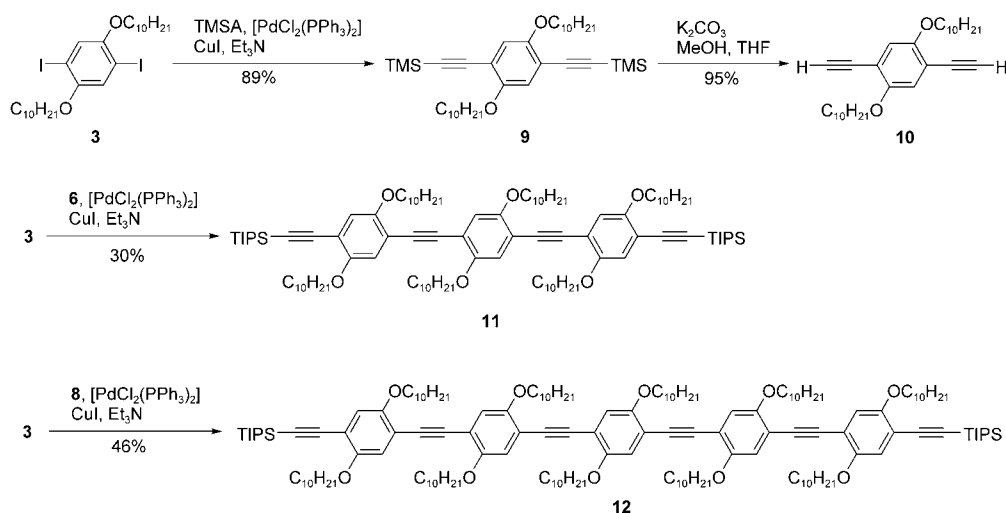
Monomeric phenyl acetylenes **9** and **10** were readily synthesized by cross-coupling and K_2CO_3 desilylation reactions (Scheme 2). For the synthesis of longer OPEs, trimer **11** and pentamer **12**, our preliminary efforts using a divergent elongation route were not satisfactory. A significant amount of oxidative homocoupling byproducts persistently formed even with vigorous exclusion of oxygen from the reaction mixture. These by-products had similar R_f values on silica gel column chromatography as the products, and as a result of this, it was extremely difficult to obtain spectroscopically

pure products **11** and **12** through this approach. Alternatively, a convergent route (as laid out in Scheme 2) was carried out, and, indeed, it gave satisfactory yields for trimer **11** and pentamer **12** pure enough for NMR spectroscopic characterization.

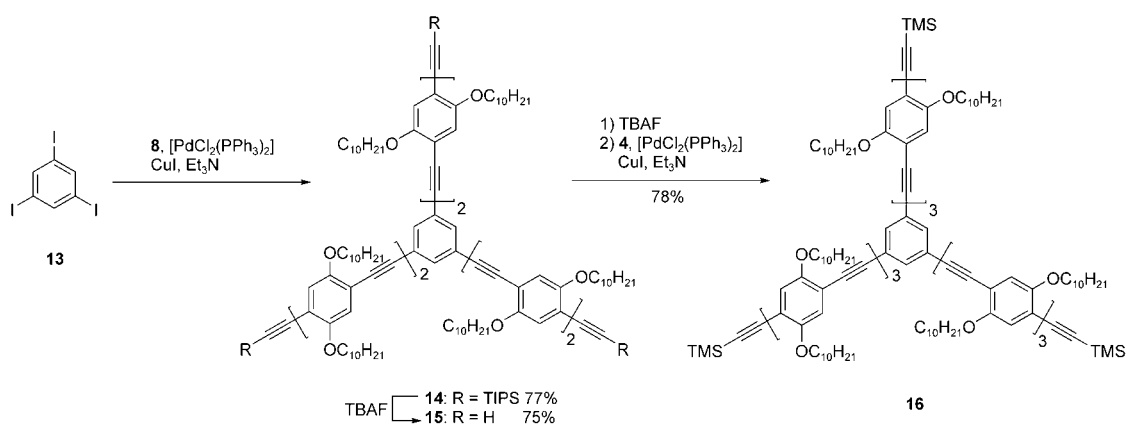
In a similar manner, a series of centrosymmetric octupolar-shaped OPE molecules **14–16** was prepared as shown in Scheme 3. 1,3,5-Triiodobenzene (**13**) was used as the central core to couple with dimer **8**, affording trigonal-shaped heptameric phenylene acetylene **14**. Removal of the TIPS groups using tetrabutylammonium fluoride (TBAF) followed by silica column separation gave terminal alkyne **15**. For a concise synthesis, compound **14** was desilylated and then coupled with compound **4** to afford decameric phenylene acetylene **16**. Interestingly, in this reaction, oxidative homocoupling was not as significant as those that occurred in the divergent

synthesis of linearly shaped OPEs (see Scheme 2). This is probably due to the increased steric hindrance in the rigid, two-dimensional OPE structure.

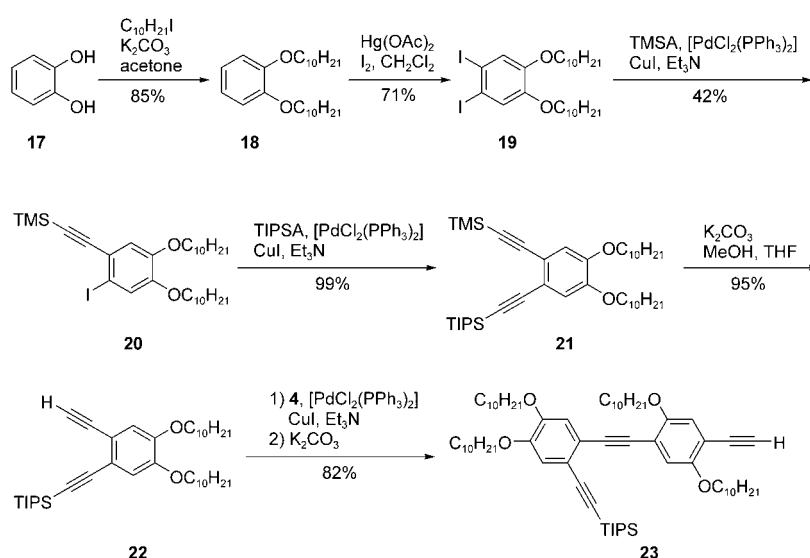
In addition to the aforementioned OPEs, we have synthesized another series of OPE molecules in which the terminal ethynylene groups are oriented at the *ortho*-position relative to the central phenylene ethynylene backbones. Schemes 4 and 5 outline the synthetic details of the *ortho*-ethynyl terminated OPEs. In Scheme 4, the building blocks **22** and **23** were readily prepared from 1,2-dihydroquinone (**17**) via a



Scheme 2. Iterative synthesis of OPEs via palladium-catalyzed coupling reactions.



Scheme 3. Synthesis of trigonal shaped OPE oligomers.



Scheme 4. Synthesis of building blocks for *ortho*-ethynylated OPEs.

synthetic approach similar to that for the previous OPE molecules (see Scheme 1).

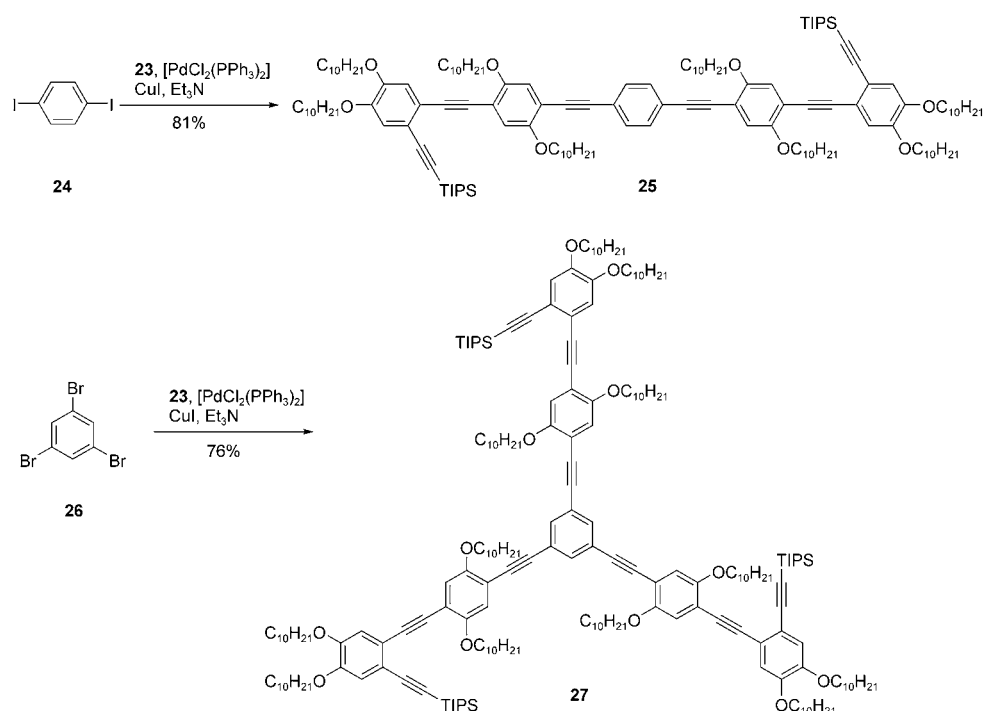
With these building blocks, we further extended the OPEs to pentamer **25** and trigonal-shaped heptamer **27**, in a convergent way, by coupling dimer **23** with 1,4-diiodobenzene (**24**) and 1,3,5-tribromobenzene (**26**) respectively. Again, since the complex molecular structures appear to increase the steric hindrance, the formation of oxidative homocoupling byproducts was diminished dramatically in these cross coupling reactions.

Synthesis of multi-[60]fullerene–OPE hybrids: With the OPE precursors in hand, we then made efforts to bond fullerene cages at the termini of each OPE framework. Initially, we followed the ethynylation procedure as described in the literature,^[38,74–77] in which lithium acetylides were first generated by *n*BuLi or *t*BuLi and then transferred into a slurry of fullerene in THF under an inert atmosphere. However, this method was found to work only for the ethynylation of

mono-terminal alkynes with fullerene, whereas the fullerene addition to multiple terminal alkyne species failed to yield the desired multiple fullerene-alkyne adducts. To solve this problem, we have devised an alternative in situ ethynylation methodology.^[72] The essence of the new ethynylation method is to add the base, lithium hexamethyldisilazide (LHMDS), slowly into a well-sonicated mixture of fullerene and terminal alkynes in THF. In this way, LHMDS can generate the lithium acetylide species in situ, which then quickly undergoes the fullerene addition reaction to form the desired ethynylated fullerene compounds. The reaction

proceeds smoothly at ambient temperature under an inert gas environment, and completes within 1 h in general. Careful removal of oxygen and moisture is essential to a successful reaction. After adding LHMDS, the mixture of fullerenes develops a deep green color that is an indication that the reaction has occurred. Quenching the reaction with excess trifluoroacetic acid (TFA) then gives the desired ethynylated fullerene product. So far, in our hands, only LHMDS leads to satisfactory results, whereas many other bases such as *t*BuOK, *n*BuLi, *t*BuLi, LDA, and LTMP have not produced any positive results.

To shed more light on the reaction mechanistically, a blank test was carried out in which LHMDS was added into a slurry of fullerene in THF (for experimental details see the Supporting Information). The reaction slowly turned green, similar to that observed in fullerene–ethynylation reactions. In the meantime, the solubility of the fullerene slurry appeared to somewhat improve. After quenching with TFA, the reaction mixture was separated into two fractions

Scheme 5. Synthesis of *ortho*-ethynylated OPE oligomers.

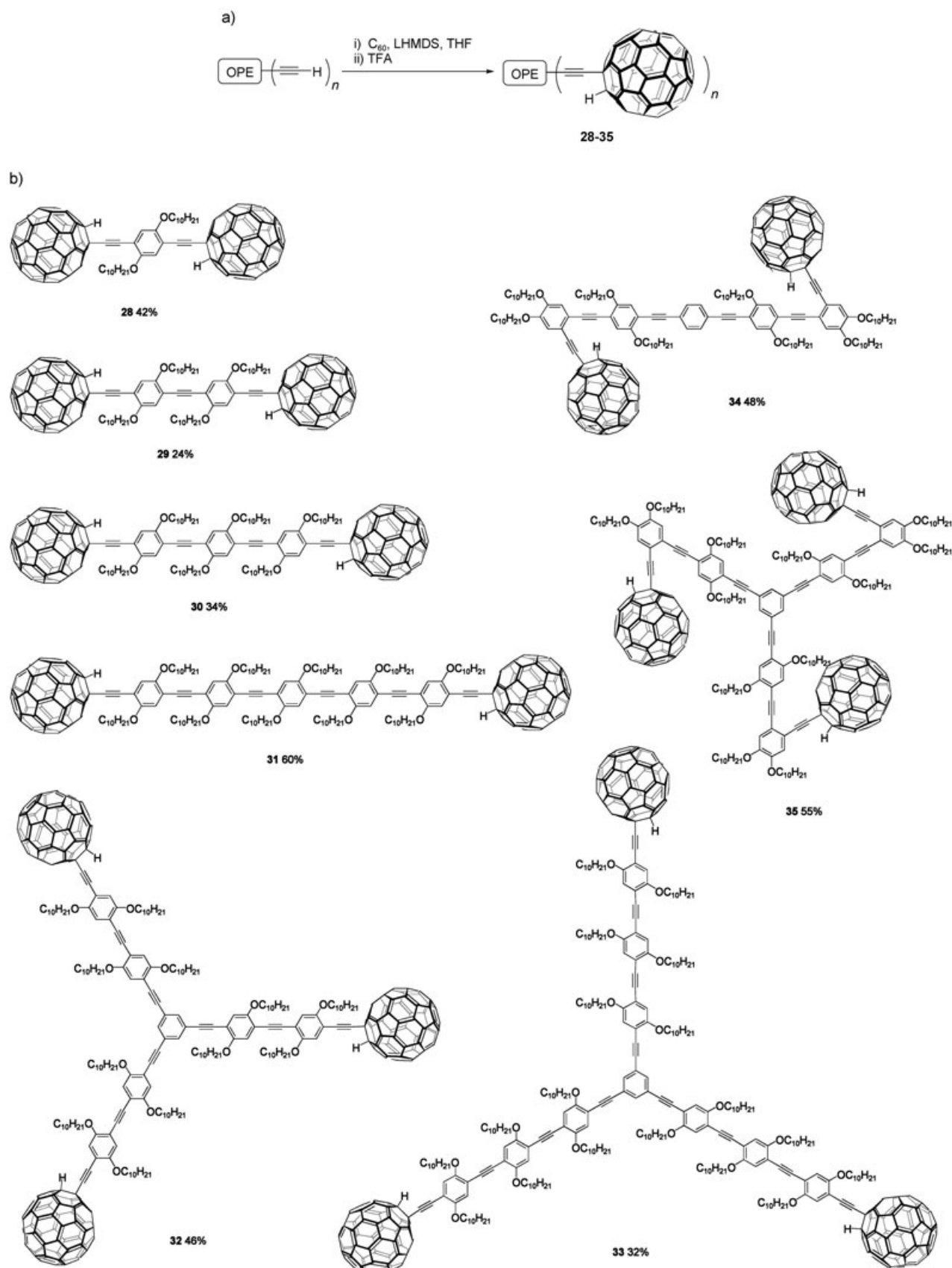
by passing it through a short silica plug. Pristine fullerene was recovered in greater than 90% yield as the first fraction, while, in the second fraction, a trace amount of a brownish solid was obtained and characterized by 1H NMR and MALDI-TOF mass spectrometry. In the 1H NMR spectrum, resonance peaks at 6.96 ppm were observed, which suggests the presence of protons directly attached to fullerene cages. However, the resonance pattern shows that it is a mixture of several compounds rather than one pure product. Therefore, it is difficult to deduce further structural information from the 1H NMR spectrum. The MALDI-TOF mass spectrum clearly shows several ion peaks at m/z 738, 760, 782, and 1001, which are probably from the fullerene adducts formed in the blank test reaction. Possibly, the peaks at m/z 738 and 782 are due to the adduct ions of $[C_{60}+NH_4]^+$ and $[C_{60}+Si_2H_6]^+$, whereas the other two are unidentifiable. According to these data, it is reasoned that the base LHMDS might interact with fullerene to solvate and stabilize the reaction intermediates, which in turn facilitates the fullerene addition reaction.

Through this *in situ* ethynylation approach, we were able to synthesize the multiple-fullerene terminated OPEs directly from respective OPE precursors. Although it is advantageous to use purified terminal alkynyl OPE precursors to produce higher yields and easier purification, we have found that in some cases the silyl-deprotected OPEs could be directly used in the fullerene ethynylation, after a brief aqueous workup, without significantly lowering the yields. However, it is worth pointing out that if the amount of impurities in the deprotection reaction is high, the mixture should be purified before carrying it forward. Otherwise, the subse-

quent column purification of fullerene products would be problematic. The synthetic details and yields for the fullerene–OPE hybrids **28–35** are listed in Scheme 6.

Spectrometric and NMR spectroscopic characterization: Affirmative evidence on the formation of high molecular weight OPEs and their multiple fullerene adducts was obtained from MALDI-TOF mass spectrometric analysis. The molecular ion peaks for alkyloxyated OPE precursors can be readily observed with dithranol as the matrix and the instrument operating in the linear mode. For the fullerene–OPE hybrids, in some cases, using the dithranol matrix resulted in poor molecular ion signals. Alternatively, by using sulfur as the matrix improved the spectrum quality. Molecular ion peaks, together with signals due to fragmentation, were clearly observed in all of the mass spectra of new compounds. As an example, the molecular ion peak of compound **33** is observed at m/z 6021, which represents the highest molecular weight of multi-fullerene species we have made to date.

1D and 2D NMR spectroscopic analyses provide detailed and crucial information establishing the molecular structures of the OPE precursors and their fullerene derivatives. Fortunately, the fullerene derivatives **28–35** are sufficiently soluble for NMR analysis; the solubilizing alkyloxy chains significantly interrupt the intermolecular aggregation between fullerenes. However, the signal overlap in the aromatic and alkyl regions somewhat limits spectral assignments. 1H and ^{13}C NMR data for the 2,5-dialkyloxy-*p*-phenylene ethynylene moiety have been reported for numerous small compounds and polymers,^[78a–m] but detailed assignments for sim-



Scheme 6. Synthesis of multi-[60]fullerene-OPE hybrids by an in situ ethynylation method.

ilar but symmetrically inequivalent sites in such oligomers apparently have not been reported. Of particular relevance are the NMR data reported for trimers similar to **11** and **30** and pentamers similar to **12** and **31** but differing in the length of the alkoxy side chains and the nature of the end groups.^[78e,i]

To better understand the magnetic shielding properties of the OPE precursors and fullerene derivatives, a thorough NMR study was conducted on these compounds. A 500 MHz spectrometer can easily resolve the proton and carbon resonances from the OPE backbone of compounds as complex as **11**, where, for example, three aromatic proton signals, nine aromatic carbon signals, four alkynyl carbon signals, and three -OCH₂- carbon signals are clearly observed. In the corresponding fullerene derivative **30**, two of the aromatic C-H carbon signals overlap, but remarkably, all 30 fullerene sp² signals are resolved. The ¹H and ¹³C signal assignments for **30** are shown in Figure 1 and listed in Table 1. The aromatic carbons bonded to H_b and H_d give

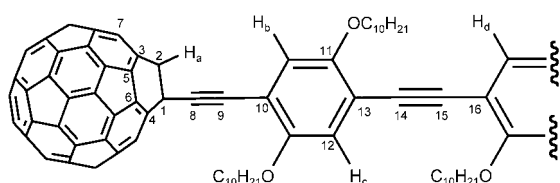


Figure 1. Assignments (Table 1) of ¹H and ¹³C NMR resonances for compound **30** based on long-range proton-carbon couplings, 2D NMR experiments, and calculated ¹³C shifts for C₆₀H(C≡CH).^[77] The assignments for C5, C6, and C7 are tentative.

Table 1. ¹³C and ¹H NMR Assignments.

Assignment	Resonance (ppm)
C1	55.43
C2	61.93
C3	151.46
C4	151.34
C5	136.07
C6	135.08
C7	142.09
C8	97.47
C9	80.56
C10	115.17
C11	154.33
C12	116.71
C13	112.78
C14	91.66
C15	92.18
C16	114.31
H _a	7.14
H _b	7.21
H _c	7.05
H _d	6.98

overlapping signals at δ 117.10, while the aryloxy carbon signals at δ 153.38 and 153.39 cannot be assigned to specific sites. In addition, a ¹H-coupled ¹³C spectrum of **30** displays

all 13 long-range couplings up to five bonds from the fullerene proton to the fullerene sp² carbons. In comparison, no more than five such couplings have previously been reported in other C_s symmetry C₆₀HR species bearing one proton and one adjacent functional group.^[78n,o]

In the ¹³C NMR spectra of some of the longer OPE compounds, aromatic C-H or C-O signals sometimes overlap, but the alkynyl carbon signals remain resolved. Compound **34** is remarkable in that six different signals are observed for the fullerene proton and five types of aromatic protons, and all of the OPE backbone carbon signals are resolved. Detailed chemical shift assignments for **30**, **34**, and other compounds could be made through a combination of 1D (¹H, ¹³C with and without ¹H decoupling, and DEPT-135 ¹³C) and 2D (¹H,¹H COSY, ¹H,¹³C HSQC, and ¹H,¹³C HMBC) NMR experiments, as described in detail in the Supporting Information.

Electronic absorption properties: The electronic absorption characteristics of OPE oligomers and their fullerene derivatives were studied by UV/Vis spectroscopy in *o*-dichlorobenzene solutions. In the normalized UV/Vis spectra of linear fullerene-OPEs **28–31** (Figure 2a), a bathochromic shift of absorption maxima, λ_{max} , is observed. A similar shift is seen in the UV/Vis spectra of their OPE precursors **7**, **9**, **11**, and **12** (Figure 2b), which suggests that the bathochromic shift in the fullerene-OPEs is mainly due to the increasing π conjugation path in the OPE backbones. By extrapolation, these shifts are predicted to reach saturation by the heptamer or octamer stage, which is in agreement with previous studies of OPEs.^[78p] There is a significant increase in the absorption intensity in the high-energy absorption region (ca. 315 nm) for fullerene compounds **28–31** in comparison with their counterpart OPEs' spectra and that of pristine C₆₀. It is reasonable to believe that this enhancement is due to the contribution from fullerene groups; most likely due to an electronic transition from the orbitals of OPE to those of the fullerene cages. Although electrochemistry results suggest that inductive effects might be present in these fullerene derivatives (see below), such effects cannot be clearly confirmed by the low-energy absorption band in the UV/Vis spectrum since the characteristic hump of the fullerene cage (ca. 432 nm), along with its tail, hinders confirmative analysis.^[77] Nevertheless, in the region above 450 nm of the spectrum, distinctively enhanced absorption tails are observed in a consistent pattern for fullerene-OPE hybrids **28–31**. These absorption bands differ from the UV/Vis patterns obtained by simply summing the UV/Vis curves of pristine fullerene and respective OPE oligomers (see Supporting Information). Likely, these absorptions are due to the relatively weak electronic interactions between fullerene cages and OPE backbones. Despite being connected by a conjugated OPE bridge, an absorption band from intramolecular electronic interaction between the fullerene groups is not detected.

The UV/Vis spectra of the octupolar fullerene-derivatives **32** and **33** are shown in Figure 3a. There is a substantial red-

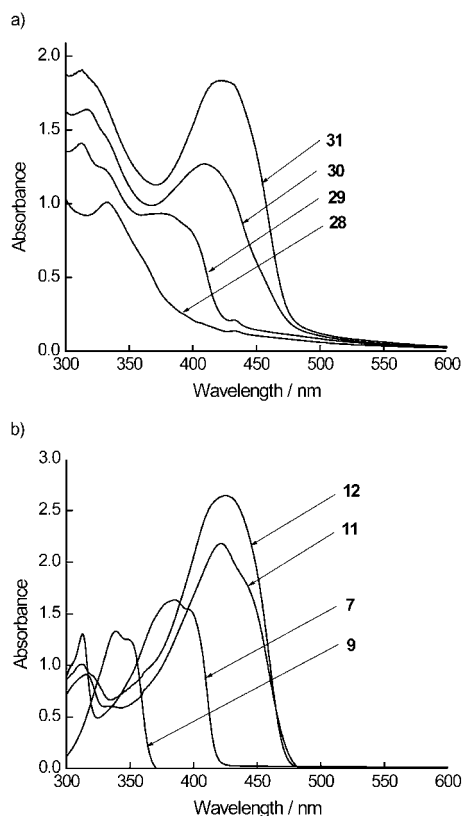


Figure 2. UV/Vis spectra of a) linear bis(fullerenyl)-OPEs **28–31** in comparison with b) OPE precursors **7**, **9**, **11**, and **12**.

shift of the λ_{max} value by about 10 nm from compounds **32** to **33**, which is comparable to the shift observed in the spectra of their OPE precursors **14** and **16**. This comparison suggests that the red-shift is primarily due to the extension of the π delocalization path in the OPE moieties. Again, the long tails from 450 to 600 nm that are characteristic absorptions of fullerene moieties are seen in the UV curves of **32** and **33**. The *ortho*-terminal-alkynylated fullerene–OPE species **34** and **35** show similar UV/Vis profiles (Figure 3a) with respect to their precursors **25** and **27** (Figure 3b). A slight shoulder at 430 nm in the UV profile of **35** is consistent with the functionalized fullerene absorption peaks observed in the spectra of **28** and **29**.

Cyclic voltammetry studies of [60]fullerene–OPE hybrids:

The electrochemical behavior of multiple fullerene–OPE hybrids **28–33**, and **35**, in solutions of *o*-dichlorobenzene at room temperature with Bu_4NBF_4 as the electrolyte, were characterized by cyclic voltammetry (CV). The most pronounced feature of the CV profiles for the *para*-oriented fullerene–OPEs **28–33** is the close resemblance to that of pristine fullerene. Figure 4 shows the selected cyclic voltammograms in comparison with pristine fullerene. Although there are possible electronic interactions between the fullerene moieties, only three couples of reversible redox waves are observed in the accessible potential window of the solvent under the present conditions for compounds **28–33** and **35**. These results indicate that there is no electronic interaction

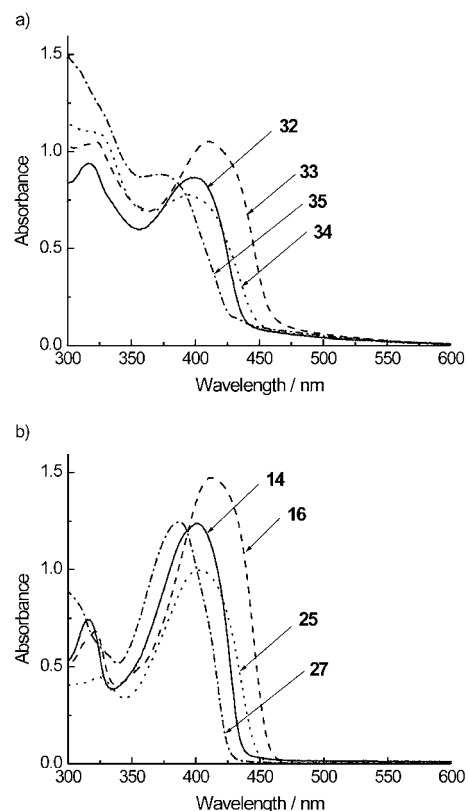


Figure 3. UV/Vis spectra of a) multi-[60]fullerene-OPEs **32–35** in comparison with b) OPE precursors **14**, **16**, **25**, and **27**.

between fullerene moieties on the CV time scale—a conclusion that is consistent with the earlier report on acetylene-connected dumbbell-type fullerenes.^[66–68] Detailed redox potential data of **28–33** and **35** are summarized in Table 2. No well-defined reversible redox waves were observed in the positive potential region (selected CV spectra in Supporting Information). The three well-defined redox waves (I, II, and III in Figure 4) observed for all listed compounds shift toward more negative potentials relative to pristine fullerene. This is because of the predominantly inductive electronic interactions from the electron-rich OPE moiety and/or the decrease of π delocalization on the fullerene cage due to the introduction of two sp^3 carbon atoms. For the linear multi-fullerene–OPEs **28–31**, the formal potentials of the first redox wave I shift cathodically with the increasing chain length of the OPE. This observation strongly suggests the existence of electronic interplays between fullerenes and OPE moieties, and is further consistent with the UV/Vis results. The cyclic voltammogram of *ortho*-alkynylated compound **35** shows features similar to the other fullerene derivatives, except that the second and third formal potentials of **35** are the least negative among them (Table 2). Likely, this is due to the enhanced inductive effects since the fullerenes and OPEs are oriented closer to each other in **35**.

Third-order optical nonlinearities and two-photon absorption properties: Third-order nonlinear optical (NLO) properties of organic systems are at the forefront of photonics

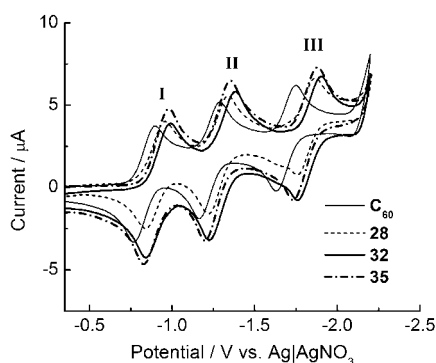


Figure 4. Cyclic voltammograms of C_{60} , and **28**, **32** and **35** in 0.1 M Bu_4NBF_4/o -dichlorobenzene at a scan rate of 0.01 V s^{-1} at room temperature.

Table 2. Results of the cyclic voltammetry measurements.

Compound	Formal potential ^[a] , $E_{1/2}$ [V]		
	I	II	III
C_{60}	-0.832	-1.227	-1.691
28	-0.901	-1.281	-1.813
29	-0.905	-1.288	-1.814
30	-0.906	-1.286	-1.813
31	-0.909	-1.292	-1.814
32	-0.918	-1.304	-1.831
33	-0.906	-1.299	-1.846
35	-0.906	-1.274	-1.807

[a] Formal potentials are calculated as averages of oxidation and reduction potentials. Potentials are given in Volts ($\pm 0.003 \text{ V}$) versus a non-aqueous reference electrode, $Ag/AgNO_3$. The formal potential of 2 mm ferrocene in 0.1 M Bu_4NBF_4 and acetonitrile is 70 mV versus this $Ag/AgNO_3$ reference electrode.

research for technological applications. Finding high-transparency materials with appropriately large ultrafast hyperpolarizabilities, γ , is desired for all-optical switching applications.^[79] Moreover, the imaginary component of third-order susceptibilities determines the molecular two-photon absorption (TPA) cross-section, $\sigma^{(2)}$ an optical property potentially useful for optical power limiting,^[80,81] upconverted lasing,^[82] two-photon fluorescence spectroscopy,^[83] three-dimensional optical memory and microfabrication,^[84–88] as well as photodynamic therapy.^[89] In general, TPA refers to a molecular process in which the simultaneous absorption of two photons promotes an electron to an energy level at the photons sum-energy.^[90] The efficiency of this process is characterized by the TPA cross section $\sigma^{(2)}(\omega)$, which is related to $\text{Im}(\gamma)$ by Equation (1):^[91]

$$\sigma^{(2)} = ((8\pi^2 h\omega^2)/(n^2 c^2))L^4 \text{Im}\gamma(-\omega, \omega, \omega, -\omega) \quad (1)$$

where h is Planck constant, n is the refractive index, c is the speed of light, ω is the frequency of the light, and L is the local field factor.

Possessing a dense network of delocalized π electrons, as well as high-transparency in the near- and mid-infrared, full-

erenes are appealing candidates for NLO applications.^[92,93] NLO research on pristine C_{60} has proved disappointing, as unfunctionalized fullerenes display miniscule hyperpolarizabilities and poor solubility.^[94–96] Functionalized fullerenes, however, have been shown to yield large γ and $\sigma^{(2)}$ values.^[33,97–99] By bonding fullerenes to conjugated oligomers such as OPEs, the electronic characteristics of both components are altered, thus modifying the overall NLO properties. Therefore, it is of particular interest to shed light on the fullerene-controlled third-order NLO behavior as well as respective structure–property relationships. From a geometry standpoint, the OPE symmetries investigated in this work are also of particular interest for NLO research, with the effects of both extended conjugation and polar/multipolar symmetries on the NLO properties of molecular systems being investigated herein.^[100–110] In the OPE-based compounds that we have studied, both quadrupolar (linearly π -conjugated C_{60} - π - C_{60}) and octupolar (cross-conjugated) systems with similarly conjugated backbones are investigated.

For third-order NLO measurements, we used a differential optical Kerr effect (DOKE) detection technique, described elsewhere.^[73] In brief, DOKE is an ultrafast pump-probe technique that uses an intense linearly-polarized (pump) pulse to induce nonlinearities in the sample that are consequently probed by a weaker, degenerate, circular-polarized (probe) pulse. By varying the input polarization of the pump pulse with respect to the analyzed polarizations of the probe pulse, we can obtain the time-resolved real (birefringent) and imaginary (nonlinear absorption) components of the sample's third-order optical nonlinearities. Our pulses are generated by an amplified Ti/sapphire laser producing 800 nm, 90 fs pulses at a 1 kHz repetition rate.

Preliminary efforts to investigate short fullerene-OPE chains **28**, **29**, and pristine C_{60} failed due to their low solubility in organic solvents. The inability to resolve nonlinearities of dilute C_{60} solutions is consistent with prior findings that pristine fullerenes display extremely small nonlinearities.^[94–96,111] On the other hand, fullerenes bonded to long-chain OPEs should be more soluble and were primarily targeted in our study. Compounds **31** and **32** were selected as potential candidates for NLO investigation, since they represent not only multiple-fullerene derivatives but also two different types of molecular dimensionalities, that is, linearly π -conjugated (quadrupolar) and cross-conjugated (octupolar) structures respectively. To determine the effects of fullerene terminal groups in governing the third-order NLO properties, the corresponding OPE compounds **12** and **14** were also investigated. For NLO studies, all samples were analyzed in CH_2Cl_2 solutions. Both compounds **31** and **32** are weakly soluble in CH_2Cl_2 . Whereas a dilute solution of **31** ($< 2 \text{ mM}$)^[112] gave detectable signals, **32** was not soluble enough for accurate measurements, with a saturated solution (ca. 0.5 M) yielding an unresolvable response. Although CS_2 is a better solvent for fullerene compounds, CH_2Cl_2 displays both smaller and faster nonlinearities that allow for the extraction of small solute-derived signals with far better resolution.

In Table 3, γ and $\sigma^{(2)}$ values for the OPE sample series are listed. All γ values are presented with respect to a reference value of 5.2×10^{-37} esu for THF.^[73] $\sigma^{(2)}$ values are presented with respect to a reference (DOKE) value of $380 \times 10^{-50} \text{ cm}^4 \text{ s}^{-1} \text{ molecule}^{-1}$ of MPPBT,^[113] a diacetylene-based chromophore used as a reference for all our nonlinear-absorption scans. Fullerene-terminated sample **31** displays the largest molecular hyperpolarizability of $\gamma = 10 \times 10^{-34}$ esu. This is a relatively large nonlinearity for a conjugated molecule in solution, investigated nonresonantly by femtosecond Kerr spectroscopy, and compares well with other ultrafast third-order NLO studies of fullerene derivatives.^[94,98] Of compounds **12**, **14** and **31**, compound **31** also has the largest TPA cross-section, with $\sigma^{(2)} = 140 \times 10^{-50} \text{ cm}^4 \text{ s}^{-1} \text{ molecule}^{-1}$. This value is large for a non-polymeric compound studied with femtosecond pulses, and displays a value that compares well with the only other fullerene-derivative TPA results reported in the literature, studied with nanosecond pulses.^[82,97,103,114]

Table 3. Molecular third-order hyperpolarizabilities γ , TPA cross sections $\sigma^{(2)}$, and low-energy absorption peak wavelengths for compounds **12**, **14**, and **31**. ($\sigma^{(2)}$ values are relative to $380 \times 10^{-50} \text{ cm}^4 \text{ s}^{-1} \text{ molecule}^{-1}$ of MPPBT in DMSO).

Compound	Concentration [mM]	λ_{max} [nm]	γ [10^{-34} esu]	$\sigma^{(2)}$ [$10^{-50} \text{ cm}^4 \text{ s}^{-1}$]
12	20	430	5.7 ± 0.4	65 ± 10
14	20	415	4.4 ± 0.2	28 ± 8
31	2	425	10 ± 3	140 ± 40

Aside from absolute NLO coefficient values (the comparison of which can be misleading^[115,116]) we find several interesting trends in our data: Fullerene-terminated OPE **31** shows a γ value that is nearly twice that of its OPE precursor **12**. Likewise, a two-fold enhancement in $\sigma^{(2)}$ is observed, when comparing compound **31** with **12**. A similar doubling of the two-photon coefficients of conjugated chromophores upon attaching a terminal fullerene is reported by Chiang et al.^[97] Considering that pristine fullerenes display negligible nonlinearities, it is possible that this enhancement of γ and $\sigma^{(2)}$ for **31** compared with **12** is due to periconjugation effects and/or charge transfer from OPE to fullerene in the excited state. In previous works, Chiang et al., as well as others, attribute the sizable TPA response of functionalized fullerenes to charge transfer from the conjugated backbone to the terminal fullerene that acts as an electron acceptor.^[33,94,97,98,111,117] This explanation is consistent with our NLO and UV/Vis results. That same study, however, found that an octupolar conjugated backbone geometry displays larger $\sigma^{(2)}$ values than a linear conjugated quadrupolar conjugated backbone. In contrast, we find that the quadrupolar **12** displays a larger TPA cross-section than the octupolar **14**. This is, perhaps, not surprising when we consider that although the through-centre arms of these compounds have the same number of OPE units, in the octupolar geometry,

linear conjugation is interrupted by the meta-linked central phenyl ring (i.e., cross conjugation), whereas the quadrupolar molecule is fully conjugated along its length.^[107] On the other hand, other groups have synthesized octupolar molecules with an amide core that has been shown to allow some degree of conjugation through the center.^[107,118,119] Moreover, the superiority of the γ values of **12** over **14** further suggests that the degree of π delocalization plays a more crucial role than the (multi)polar symmetry in controlling the NLO behavior of the molecules synthesized here.

In addition to instantaneous two-photon absorption, the TIPS-terminated OPEs also display excited-state absorption (ESA).^[91,120] The DOKE layout is only sensitive to changes in the probe beam. TPA is recorded when one photon is absorbed from each of the pump and probe beams. This can only occur when the beams are overlapped temporally. For excited-state absorption, two photons are simultaneously absorbed from the intense pump beam to a high-lying two-photon state. After relaxation to a lower-lying excited state, a photon may be absorbed from the probe beam. This process will depend on the relaxation dynamics from the two-photon and lower excited-state as well as the transition probability of the excited state from which the subsequent absorption is to take place.^[91,120]

Figure 5 presents the time-resolved nonlinear absorption responses of **12**, **14**, **31**, and MPPBT. CH_2Cl_2 , lacking TPA only, displays a very small transient grating signal typical of coherent coupling (not shown).^[121] Whereas OPE compounds **12** and **14** both display a measure of excited-state absorption, the fullerene-terminated **31** shows only instantaneous TPA. When the nonlinear absorption of MPPBT is shown for comparison, it becomes clear that the excited-state dynamics of both the quadrupolar OPE **12** and octupolar OPE **14** are quite similar (Figure 5b). This is somewhat surprising as the electronic levels in these systems are expected to be closely governed by the transition dipoles and geometry. For example, the lowest lying energy state in the centrosymmetric **12** is expected to be two-photon forbidden, while having a higher-energy state that is one-photon forbidden but two-photon allowed. On the other hand, the non-centrosymmetric **14** is expected to have both a one- and two-photon allowed first excited state.^[105,107] Because the band-gap wavelength ($\lambda_{\text{max}} = 415\text{--}430$ nm) of these samples is longer than the two-photon wavelength ($1/2 \lambda_{\text{laser}} = 400$ nm), it is possible that the TPA is occurring to a high-lying excited state. Accordingly, from the UV/Vis spectra and time-resolved ESA dynamics, it is reasonable to suggest that it is the OPE chromophore units themselves, rather than the multipolar geometry, that regulates the excited-state behavior of samples **12** and **14**. The fact that the OPE precursor **12** displays excited-state absorption while the fullerene-terminated compound **31** does not, is further consistent with a charge-transfer mechanism, in which relaxations from the two-photon to the ground state take place without significant population of the intermediate excited state that is observed in **12** and **14**.^[97] However, in the absence of two-photon induced fluorescence spectroscopy data^[90] it is diffi-

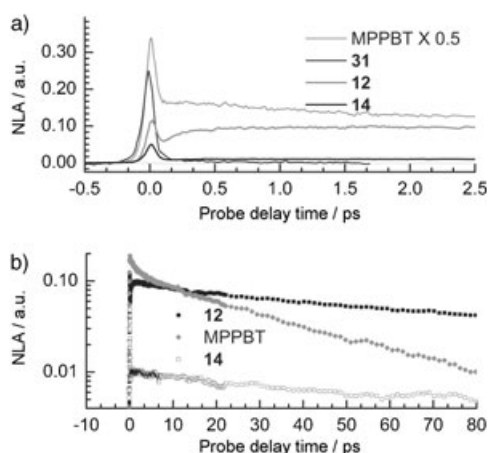


Figure 5. Time-resolved (molecular) nonlinear absorption response of **31**, **12**, **14**, and MPPBT. The MPPBT response has been scaled down by 50% for ease of comparison. a) Two-photon absorption is seen on-peak ($t = 0$ ps) for all samples, while longer time scales represent excited-state absorption (ESA). Note that ESA is absent in the fullerene-terminated OPE **31**. b) (Log-linear graph) Excited-state absorption decays, showing that samples **12** and **14** have strikingly similar relaxation dynamics.

cult to conclusively map out the electronic states in these samples.

Conclusion

We have developed a new in situ alkylation methodology that allows fullerene to be functionalized with a variety of terminal alkynes in satisfactory yields. The protocol is particularly useful for generating various multi-fullerene containing compounds, and thus widens the synthetic capability in the design and preparation of new fullerene derivatives. In this context, we have synthesized a number of multiple-fullerene OPE hybrid molecules. The high purity of the products obtained enables the detailed characterization of the NMR features of the functionalized fullerene cages as well as the carbon-rich OPE backbones by 1D and 2D NMR studies. Electronic properties of these new fullerene-OPE derivatives have been probed by UV/Vis spectroscopic analysis, which suggests the existence of electronic interactions between the fullerene and OPE components of the molecule. This is further supported by electrochemical studies using the CV method. The observation that the formal potentials of the first redox wave consistently shift toward the negative direction as the OPE chain length increases is an important piece of evidence for the interplays between the fullerenes and OPE moieties. Furthermore, we investigated the third-order NLO and nonlinear-absorption properties of fullerene derivative **31** and OPE precursors **12** and **14** by using a DOKE detection technique. The measured γ and $\sigma^{(2)}$ values for fullerene derivative **31** are approximately double those of its OPE precursor **12**, whereas pristine C_{60} nonlinearities are negligible. This provides further evidence that a synergistic interaction between the conjugated OPE

backbone and terminal fullerenes is taking place. Other groups have attributed similar findings to the formation of a charge-transfer species in which excited electrons pass from the conjugated backbone to the terminal fullerene. This proposed mechanism is further supported by the comparisons of the excited-state absorption dynamics of compounds **12**, **14** and **31**. Whereas both of the pure OPE frameworks display similar excited-state absorption, end-capping with fullerene (in **31**) yields a compound that only displays instantaneous two-photon absorption. Finally, the fullerene-terminated OPE **31** displays sizable γ - and $\sigma^{(2)}$ -values that are consistent with other C_{60} derivatives reported in the literature. Thus, our findings are potentially instructive to guiding the molecular design and engineering of organic-based electronic and nonlinear optical materials.

Experimental Section

General: All reactions were performed under an atmosphere of nitrogen unless stated otherwise. Precursors **2–15** and multiple [60]fullerene derivatives **28–32** were available from previous studies (see Supporting Information).^[72] Precursors **18** and **19** were prepared according to literature procedures.^[122] Reagent grade diethyl ether and tetrahydrofuran (THF) were distilled from sodium/benzophenone. Triethylamine (TEA) was distilled over CaH_2 . Fullerene (99.5+ % pure) was purchased from MTR Ltd. and used as received. LHMDS (1 M solution in THF) and TBAF (1 M solution in THF) were obtained from Aldrich. Flash column chromatography was performed using 230–400 mesh silica gel from EM Science. Thin layer chromatography was performed using glass plates pre-coated with silica gel 40 F_{254} purchased from EM Science. 1H and ^{13}C NMR spectra were recorded on Bruker Avance-400 and 500 spectrometers. 2D-NMR experiments ($^1H, ^1H$ COSY, $^1H, ^{13}C$ HSQC, and $^1H, ^{13}C$ HMBC) were conducted on the Bruker 500 spectrometer. FT-IR spectra were measured on a Perkin–Elmer 1600 series instrument. Electron impact mass spectra were recorded on a Finnigan MAT95 mass spectrometer and MALDI-TOF mass spectrum was performed on a Bruker BiFlex-III MALDI mass instrument. Melting points were measured on a Mel-Temp instrument (uncorrected). UV/Vis spectra were recorded on a Shimadzu UV-3101PC spectrometer. Ultra-sonicated fullerene slurry in THF was prepared in a general ultrasonic cleaner.

General procedure for the coupling of a terminal alkyne with an aryl halide using a palladium-catalyzed cross-coupling (Sonogashira) protocol: The aryl halide, the terminal alkyne, $PdCl_2(PPh_3)_2$ (ca. 5 mol% per aryl halide), and CuI (ca. 10 mol% per aryl halide) were added to an oven-dried round bottom flask equipped with a magnetic stir bar. A solvent system of TEA and/or THF was added depending on the substrates. Upon completion of the reaction, it was quenched with a saturated solution of NH_4Cl . The organic layer was then diluted with hexanes, diethyl ether or CH_2Cl_2 , and washed with water or saturated NH_4Cl (1 \times). The combined aqueous layers were extracted with hexanes, diethyl ether or CH_2Cl_2 (2 \times). The combined organic layers were dried over $MgSO_4$ and the solvent was removed in vacuo to afford the crude product, which was purified by column chromatography (silica gel). Eluents and other slight modifications are described below for each compound.

General procedure for the addition of C_{60} to terminal alkynes using LHMDS: The terminal alkyne and C_{60} (2 equiv per terminal alkyne H) was added to an oven-dried round bottom flask equipped with a magnetic stirrer. After adding THF, the flask was sonicated for at least 3 h. To the greenish-brown suspension formed after sonication was added LHMDS drop-wise at room temperature. As the reaction progressed, the mixture turned into a deep greenish-black solution. During the addition of the LHMDS, small aliquots from the reaction were extracted and quenched with trifluoroacetic acid (TFA), dried, and re-dissolved in CS_2

for TLC analysis (developed in a mixture of CH_2Cl_2 and hexanes). Completion of the reaction was confirmed by the disappearance of the starting materials. The reaction was usually complete within 0.5–1.5 h. Upon completion of the reaction, it was quenched with TFA to give a brownish slurry. Excess TFA and solvent were then removed in vacuo to afford a crude product that was purified by flash column chromatography (silica gel). Eluents and other slight modifications are described below for each compound.

Compound 16: TBAF (0.32 mL, 0.32 mmol) was added to a solution of **14** (328 mg, 0.106 mmol) in THF (5 mL). After stirring at RT for 5 min, the reaction was quenched with H_2O and extracted with diethyl ether. After a brief aqueous workup, the solvents were removed in vacuo. The resulted desilylated product was coupled with **4** (260 mg, 0.424 mmol) under catalysis of $[\text{PdCl}_2(\text{PPh}_3)_2]$ (12 mg, 0.017 mmol) and CuI (6 mg, 0.03 mmol) in Et_3N (40 mL) following the general coupling procedure. After reaction the residue was purified by silica column chromatography with 50–60% CH_2Cl_2 in hexanes to afford **16** (337 mg, 78%) as a yellow solid. $^1\text{H NMR}$ (500 MHz, CDCl_3): δ = 7.64 (s, 3H), 7.03 (s, 3H), 7.013 (s, 3H), 7.008 (s, 6H), 6.96 (s, 3H), 6.95 (s, 3H), 4.03 (m, 24H), 3.97 (m, 12H), 1.86 (m, 36H), 1.51 (m, 36H), 1.41–1.16 (m, 216H), 0.93–0.78 (m, 54H), 0.27 ppm (s, 27H); $^{13}\text{C NMR}$ (125 MHz, CDCl_3): δ = 154.4, 154.0, 153.72, 153.71, 153.68, 153.5, 134.1, 124.4, 117.6, 117.5, 117.4, 117.2, 115.0, 114.8, 114.53, 114.47, 113.9, 113.7, 101.4, 100.3, 93.5, 91.9, 91.8, 91.7, 87.4, 70.0, 69.9, 69.6, 32.13, 32.11, 31.97, 29.92, 29.87, 29.84, 29.80, 29.71, 29.69, 29.67, 29.59, 29.57, 29.52, 20.39, 26.34, 26.29, 26.25, 26.21, 26.18, 23.1, 22.9, 22.7, 14.3, 0.19 ppm; IR (CH_2Cl_2 cast): $\tilde{\nu}$ = 2924, 2853, 2151, 1578, 1590 cm^{-1} ; MALDI-TOF MS (dithranol as the matrix): m/z : calcd for $\text{C}_{273}\text{H}_{426}\text{O}_{18}\text{Si}_3$: 4077; found: 4078 $[M]^+$.

1,2-Bis(decyloxy)-4-iodo-5-trimethylsilylethynylbenzene (20): See the general procedure for the Pd/Cu coupling reaction. The materials used were TMSA (2.20 mL, 15.5 mmol), **19**^[122] (8.83 g, 13.7 mmol), $[\text{PdCl}_2(\text{PPh}_3)_2]$ (0.25 g, 0.36 mmol), CuI (0.10 g, 0.53 mmol), TEA (20 mL), and THF (100 mL) at room temperature overnight. The residue was purified by flash column chromatography with 10% CH_2Cl_2 in hexanes to give product **20** (3.55 g, 42%) as a yellow oil. $^1\text{H NMR}$ (400 MHz, CDCl_3): δ = 7.21 (s, 1H), 6.96 (s, 1H), 3.95 (m, 4H), 1.80 (m, 4H), 1.45 (m, 4H), 1.33 (m, 24H), 0.89 (t, $^3J(\text{H,H}) = 6.7$ Hz, 6H), 0.28 ppm (s, 9H); $^{13}\text{C NMR}$ (100 MHz, CDCl_3): δ = 150.3, 149.0, 123.0, 121.9, 117.2, 107.2, 96.6, 90.8, 69.54, 69.47, 32.13, 29.81, 29.78, 29.6, 29.3, 29.25, 29.16, 26.13, 22.9, 14.3, 0.14 ppm; FTIR (CH_2Cl_2 cast): $\tilde{\nu}$ = 2954, 2923, 2855, 2153 cm^{-1} ; HRMS (EI): m/z : calcd for $\text{C}_{31}\text{H}_{53}\text{IO}_2\text{Si}$: 612.2860; found: 612.2849 $[M]^+$.

1,2-Bis(decyloxy)-4-triisopropylsilylethynyl-5-trimethylsilylethynylbenzene (21): See the general procedure for the Pd/Cu coupling reaction. The materials used were TIPSA (2.00 mL, 8.92 mmol), **20** (3.50 g, 5.71 mmol), $[\text{PdCl}_2(\text{PPh}_3)_2]$ (0.12 g, 0.17 mmol), CuI (0.054 g, 0.28 mmol), and TEA (50 mL) at 50°C overnight. The residue was purified by flash column chromatography with 10–20% CH_2Cl_2 in hexanes to give product **21** (3.77 g, 99%) as a pale yellow oil. $^1\text{H NMR}$ (400 MHz, CDCl_3): δ = 6.91 (s, 1H), 6.88 (s, 1H), 3.98 (m, 4H), 1.81 (m, 4H), 1.46 (m, 4H), 1.31 (m, 24H), 1.16 (s, 21H), 0.89 (t, $^3J(\text{H,H}) = 6.7$ Hz, 6H), 0.25 ppm (s, 9H); $^{13}\text{C NMR}$ (100 MHz, CDCl_3): δ = 149.5, 149.4, 119.3, 119.0, 117.3, 117.27, 105.9, 104.2, 96.5, 93.1, 69.6 (2 \times), 32.3, 30.0, 29.97, 29.8, 29.76, 29.5, 29.48, 26.3, 23.1, 19.2, 14.5, 11.8, 0.46 ppm; FTIR (CH_2Cl_2 cast): $\tilde{\nu}$ = 2924, 2923, 2859, 2151 cm^{-1} ; HRMS (EI): m/z : calcd for $\text{C}_{42}\text{H}_{74}\text{O}_2\text{Si}_2$: 666.5227; found: 666.5235 $[M]^+$.

1,2-Bis(decyloxy)-4-ethynyl-5-triisopropylethynylbenzene (22): Compound **21** (3.77 g, 5.65 mmol), K_2CO_3 (1.66 g, 12.0 mmol), and THF/MeOH (1:1, 80 mL) were added to a round bottom flask equipped with a magnetic stirrer. The reaction mixture was stirred for 3 h at room temperature and then quenched with satd NH_4Cl and diluted with hexanes. The organic layer was washed with water (1 \times), dried over MgSO_4 , and the solvent was removed in vacuo. The residue was purified by flash column chromatography with 10–15% CH_2Cl_2 in hexanes to give product **22** (3.19 g, 95%) as a pale yellow oil. $^1\text{H NMR}$ (400 MHz, CDCl_3): δ = 6.94 (s, 1H), 6.92 (s, 1H), 3.99 (m, 4H), 3.17 (s, 1H), 1.81 (m, 4H), 1.46 (m, 4H), 1.31 (m, 24H), 1.15 (s, 21H), 0.89 ppm (t, $^3J(\text{H,H}) = 6.7$ Hz, 6H); $^{13}\text{C NMR}$ (100 MHz, CDCl_3): δ = 149.5, 149.2, 119.8, 118.1, 116.8, 116.6,

105.3, 93.3, 82.8, 79.6, 69.4 (2 \times), 32.1, 29.8, 29.78, 29.6, 29.3, 29.26, 26.2, 26.1, 22.9, 19.0, 14.3, 11.6 ppm; FTIR (CH_2Cl_2 cast): $\tilde{\nu}$ = 3314, 2931, 2856, 2149, 2108 cm^{-1} ; HRMS (EI): m/z : calcd for $\text{C}_{39}\text{H}_{66}\text{O}_2\text{Si}$: 594.4832; found: 594.4833 $[M]^+$.

Compound 23: See the general procedure for the Pd/Cu coupling reaction. The materials used were **22** (0.85 g, 1.43 mmol), **4** (0.84 g, 1.37 mmol), $[\text{PdCl}_2(\text{PPh}_3)_2]$ (0.032 g, 0.046 mmol), CuI (0.013 g, 0.070 mmol), and TEA (17 mL) at 50°C overnight. The residue was filtered through a plug of silica gel, and subjected to the next reaction with K_2CO_3 (0.33 g, 2.39 mmol) and THF/MeOH (1:1, 34 mL). The reaction mixture was stirred for 3 h at room temperature and then quenched with satd NH_4Cl and diluted with hexanes. The organic layer was washed with water (1 \times), dried over MgSO_4 , and the solvent was removed in vacuo. The residue was purified by flash column chromatography with 20% CH_2Cl_2 in hexanes to give product **23** (1.13 g, 82%) as an orange waxy solid. $^1\text{H NMR}$ (400 MHz, CDCl_3): δ = 6.98 (s, 1H), 6.96 (s, 1H), 6.95 (s, 1H), 6.94 (s, 1H), 4.01–3.96 (m, 8H), 3.34 (s, 1H), 1.84–1.80 (m, 8H), 1.48–1.46 (m, 8H), 1.35–1.24 (m, 48H), 1.12 (s, 21H), 0.91–0.86 ppm (m, 12H); $^{13}\text{C NMR}$ (100 MHz, CDCl_3): δ = 154.3, 153.8, 149.4, 149.3, 119.3, 118.7, 118.0, 117.1, 117.0, 116.7, 115.5, 112.4, 105.9, 94.4, 93.0, 87.9, 82.3, 80.3, 69.9, 69.8, 69.5, 69.4, 32.1, 29.9, 29.84, 29.81, 29.78, 29.64, 29.57, 29.45, 29.37, 29.33, 26.2, 26.1, 22.9, 19.0, 14.3, 11.6 ppm; FTIR (CH_2Cl_2 cast): $\tilde{\nu}$ = 3313, 2923, 2853, 2147 cm^{-1} ; MALDI-TOF MS (dithranol as the matrix): m/z : calcd for $\text{C}_{67}\text{H}_{110}\text{O}_4\text{Si}$: 1007; found: 1007 $[M]^+$.

Compound 25: See the general procedure for the Pd/Cu coupling reaction. The materials used were **23** (0.27 g, 0.27 mmol), 1,4-diiodobenzene (**24**) (0.040 g, 0.12 mmol), $[\text{PdCl}_2(\text{PPh}_3)_2]$ (0.01 g, 0.013 mmol), CuI (0.003 g, 0.016 mmol), and TEA (20 mL) at room temperature overnight. The residue was purified by flash column chromatography with 25–33% CH_2Cl_2 in hexanes to give product **25** (0.203 g, 81%) as a yellow-green solid. $^1\text{H NMR}$ (400 MHz, CDCl_3): δ = 7.52 (s, 4H), 7.015 (s, 2H), 7.008 (s, 2H), 6.998 (s, 2H), 6.96 (s, 2H), 4.05–3.99 (m, 16H), 1.87–1.84 (m, 16H), 1.51–1.26 (m, 112H), 1.15 (s, 42H), 0.92–0.87 ppm (m, 24H); $^{13}\text{C NMR}$ (100 MHz, CDCl_3): δ = 153.93, 153.85, 149.4, 149.3, 131.6, 123.5, 119.4, 118.7, 117.1 (2 \times), 117.0, 116.7, 115.1, 113.6, 106.0, 94.7, 94.4, 93.0, 88.3, 88.1, 69.83, 69.79, 69.4, 69.3, 32.1, 29.9, 29.87, 29.84, 29.83, 29.80, 29.79, 29.65, 29.63, 29.57, 29.37, 29.33, 26.29, 26.25, 26.21, 26.20, 22.9, 19.0, 14.3, 11.6 ppm; FTIR (CH_2Cl_2 cast): ν = 2923, 2853, 2203, 2145 cm^{-1} ; MALDI-TOF MS (sulphur as the matrix): m/z : calcd for $\text{C}_{140}\text{H}_{222}\text{O}_8\text{Si}_2$: 2089; found: 2089 $[M]^+$.

Compound 27: See the general procedure for the Pd/Cu coupling reaction. The materials used were **23** (0.67 g, 0.66 mmol), 1,3,5-tribromobenzene (**26**) (0.022 g, 0.07 mmol), $[\text{PdCl}_2(\text{PPh}_3)_2]$ (0.006 g, 0.008 mmol), CuI (0.002 g, 0.009 mmol), and TEA (13 mL) at 75°C overnight. The residue was purified by flash column chromatography with 25–35% CH_2Cl_2 in hexanes to give product **27** (0.165 g, 76%) as a yellow waxy solid. $^1\text{H NMR}$ (500 MHz, CDCl_3): δ = 7.65 (s, 3H), 6.999 (s, 3H), 6.998 (s, 3H), 6.992 (s, 3H), 6.95 (s, 3H), 4.04–3.98 (m, 24H), 1.8 (m, 24H), 1.5 (m, 24H), 1.33–1.23 (m, 144H), 1.14 (s, 63H), 0.91–0.84 ppm (m, 36H); $^{13}\text{C NMR}$ (125 MHz, CDCl_3): δ = 153.91, 153.90, 149.3, 149.2, 134.1, 124.4, 119.4, 118.7, 117.3, 117.2, 116.9, 116.6, 115.2, 113.4, 105.9, 94.5, 93.3, 93.0, 88.1, 87.4, 69.9 (2 \times), 69.4, 69.3, 32.13, 32.12, 32.11, 29.92, 29.90, 29.88, 29.85, 29.83, 29.81, 29.791, 29.788, 29.67, 29.64, 29.62, 29.58, 29.57, 29.56, 29.36, 29.33, 26.27, 26.25, 26.21, 26.20, 22.91, 22.90, 22.89, 18.98, 14.34, 14.33, 11.6 ppm; FTIR (CH_2Cl_2 cast): $\tilde{\nu}$ = 2923, 2852, 2207, 2149 cm^{-1} ; MALDI-TOF MS (sulfur as the matrix): m/z : calcd for $\text{C}_{207}\text{H}_{330}\text{O}_{12}\text{Si}_3$: 3095; found: 3095 $[M]^+$.

Compound 33: TBAF (0.15 mL, 0.15 mmol) was added to a solution of **16** (173 mg, 0.0424 mmol) dissolved in THF (5 mL). The reaction mixture was stirred for 1 min at room temperature and then quenched with satd NH_4Cl and diluted with diethyl ether. The organic layer was washed with water (1 \times), dried over MgSO_4 , the slurry was filtered and the solvent was removed from the filtrate in vacuo. All organic residues were subject to the next reaction without further purification (see the general procedure for the addition reaction of C_{60} using LHMDs). The materials used were C_{60} (229 mg, 0.318 mmol), LHMDs (0.64 mL, 0.64 mmol), and THF (220 mL). The reaction was quenched at 1 h with TFA (0.15 mL, 2.0 mmol). Crude products were dissolved in CS_2 , mixed with silica gel,

and loaded onto a column with hexanes/CS₂/CH₂Cl₂ (100:1:1). The column was eluted with hexanes/CS₂/CH₂Cl₂ (30:70:1) to remove unreacted C₆₀, and then with hexanes/CS₂/CH₂Cl₂ (50:1:50) to afford product **33** (82 mg, 32%) as a brown solid. ¹H NMR (500 MHz, CDCl₃): δ = 7.66 (s, 3H), 7.29 (s, 3H), 7.18 (s, 3H), 7.14 (s, 3H), 7.07 (s, 3H), 7.06 (s, 3H), 7.05 (s, 3H), 7.03 (s, 3H), 4.15 (t, ³J(H,H) = 6.4 Hz, 12H), 4.07 (m, 24H), 1.98–1.83 (m, 36H), 1.70–1.50 (m, 36H), 1.45–1.14 (m, 216H), 0.91–0.80 ppm (m, 54H); ¹³C NMR (125 MHz, CDCl₃): δ = 154.6, 153.8, 153.57, 153.56, 153.55, 153.48 (6 signals from the C–O in the aromatic ring), 151.7, 151.5, 147.7, 147.4, 146.7, 146.47, 146.46, 146.3, 145.9, 145.8, 145.7, 145.52, 145.51, 145.4, 144.8, 144.6, 143.3, 142.7, 142.6, 142.2, 142.11, 142.05, 141.97, 141.74, 141.67, 140.45, 140.37, 136.2, 135.3 (30 signals from sp²-C in the C₆₀ core), 133.9 (CH on the central ring), 124.2 (substituted C on the central ring), 117.3, 117.2, 116.9, 115.2, 114.7, 114.4, 114.2, 113.5, 112.9, 97.6, 93.3, 92.0, 91.7, 91.6, 91.5, 87.2, 80.3, 69.9, 69.8, 69.7, 69.6, 69.5, 62.0 (CH in the C₆₀ core), 55.6 (quaternary sp³-C in the C₆₀ core), 32.0, 31.95, 31.943, 31.940, 31.91, 30.0, 29.845, 29.837, 29.78, 29.77, 29.74, 29.72, 29.71, 29.68, 29.66, 29.60, 29.57, 29.53, 29.52, 29.49, 29.48, 29.45, 29.43, 29.41, 29.39, 29.37, 29.35, 26.6, 26.14, 26.09, 26.06, 26.02, 22.74, 22.72, 22.70, 14.18, 14.16, 14.152, 14.146, 14.140 ppm; FTIR (CH₂Cl₂ cast): $\tilde{\nu}$ = 2923, 2852, 1505, 1464 cm⁻¹; MALDI-TOF MS (dithranol as the matrix): *m/z*: calcd for C₄₄H₄₀O₁₈: 6021; found: 6021 [M]⁺. (Additional NMR information is in the Supporting Information.)

Compound 34: Compound **25** (0.16 g, 0.077 mmol), TBAF (0.2 mL, 0.2 mmol), and THF (15 mL) were added to a round bottom flask equipped with a magnetic stirrer. The reaction mixture was stirred for 1 h at room temperature and then quenched with satd NH₄Cl and diluted with hexanes. The organic layer was washed with water (1×), dried over MgSO₄, and the solvent was removed in vacuo. All organic residues were subject to the next reaction without further purification (see the general procedure for the addition reaction of C₆₀ by using LHMDs). The materials used were C₆₀ (0.17 g, 0.23 mmol), LHMDs (0.6 mL, 0.6 mmol), and THF (100 mL). The reaction was quenched at 2 h with TFA (0.3 mL, 3.9 mmol). Crude products were dissolved in CS₂ and directly loaded onto a column with hexanes/CS₂/CH₂Cl₂ (100:1:1). The column was eluted with hexanes/CS₂/CH₂Cl₂ (100:1:1) to remove unreacted C₆₀, and then with hexanes/CS₂/CH₂Cl₂ (55:45:1) for complete removal of trace C₆₀, and finally with hexanes/CS₂/CH₂Cl₂ (75:1:25 to 40:1:60) to afford product **34** (0.12 g, 48%) as a brown solid. ¹H NMR (500 MHz, CDCl₃): δ = 7.39 (s, 4H), 7.27 (s, 2H), 7.18 (s, 2H), 7.16 (s, 2H), 7.09 (s, 2H), 6.91 (s, 2H), 4.13 (t, ³J(H,H) = 6.7 Hz, 4H), 4.09 (t, ³J(H,H) = 6.5 Hz, 4H), 4.01 (t, ³J(H,H) = 6.4 Hz, 4H), 3.88 (t, ³J(H,H) = 6.7 Hz, 4H), 1.91–1.87 (m, 12H), 1.69 (m, 4H), 1.50 (m, 12H), 1.45–1.15 (m, 100H), 0.90–0.83 ppm (m, 24H); ¹³C NMR (125 MHz, CDCl₃): δ = 153.84, 153.81, 149.6, 149.3 (4 signals from C–O in the aromatic ring), 151.7, 151.6, 147.7, 147.4, 146.6, 146.41, 146.40, 146.254, 146.245, 145.8, 145.7, 145.6, 145.5, 145.43, 145.37, 144.7, 144.5, 143.2, 142.62, 142.57, 142.09, 142.06, 142.0, 141.9, 141.7, 141.6, 140.3 (29 resolved signals from sp²-C in the C₆₀ core), 131.4 (CH on the central ring), 123.2 (substituted C on the central ring), 120.2, 117.8, 117.2, 117.0, 115.9, 115.7, 114.4, 114.1, 95.2, 94.7, 94.1, 88.8, 88.0, 83.0, 69.9, 69.6, 69.3, 69.2, 62.2 (CH in the C₆₀ core), 55.5 (quaternary sp³-C in the C₆₀ core), 31.95, 31.94, 31.93, 29.74, 29.71, 29.69, 29.67, 29.66, 29.63, 29.62, 29.61, 29.58, 29.53, 29.47, 29.45, 29.43, 29.41, 29.39, 29.38, 29.32, 29.18, 29.16, 26.20, 26.15, 26.07, 26.06, 22.75, 22.74, 22.72, 22.71, 14.22, 14.18, 14.15 ppm; FTIR (CH₂Cl₂ cast): $\tilde{\nu}$ = 2920, 2850, 2205 cm⁻¹; MALDI-TOF MS (sulfur as the matrix): *m/z*: calcd for C₂₄H₁₈O₈: 3218; found: 3217 [M]⁺. (Additional NMR information is in the Supporting Information.)

Compound 35: Compound **27** (0.16 g, 0.051 mmol), TBAF (0.2 mL, 0.2 mmol), and THF (17 mL) were added to a round bottom flask equipped with a magnetic stirrer. The reaction mixture was stirred for 1 h at room temperature and then quenched with satd NH₄Cl and diluted with hexanes. The organic layer was washed with water (1×), dried over MgSO₄, and the solvent was removed in vacuo. All organic residues were subject to the next reaction without further purification (see the general procedure for the addition reaction of C₆₀ by using LHMDs). The materials used were C₆₀ (0.16 g, 0.22 mmol), LHMDs (0.5 mL, 0.5 mmol), and THF (100 mL). The reaction was quenched at 1 h with TFA (0.2 mL, 2.6 mmol). Crude products were dissolved in CS₂ and directly loaded

onto a column with hexanes/CS₂/CH₂Cl₂ (100:1:1). The column was eluted with hexanes/CS₂/CH₂Cl₂ (100:1:1) to remove unreacted C₆₀, and then with hexanes/CS₂/CH₂Cl₂ (50:50:1) for complete removal of trace C₆₀, and finally with hexanes/CS₂/CH₂Cl₂ (75:1:25 to 65:1:35) to afford product **35** (0.13 g, 55%) as a brown solid. ¹H NMR (500 MHz, CDCl₃): δ = 7.45 (s, 3H), 7.28 (s, 3H), 7.174 (s, 3H), 7.171 (s, 3H), 7.09 (s, 3H), 6.88 (s, 3H), 4.13 (t, ³J(H,H) = 6.6 Hz, 6H), 4.09 (t, ³J(H,H) = 6.7 Hz, 6H), 4.01 (t, ³J(H,H) = 6.7 Hz, 6H), 3.87 (t, ³J(H,H) = 6.7 Hz, 6H), 1.92–1.87 (m, 18H), 1.65 (m, 6H), 1.53 (m, 18H), 1.45–1.12 (m, 150H), 0.90–0.87 (m, 27H), 0.80 ppm (t, ³J(H,H) = 7.0 Hz, 9H); ¹³C NMR (125 MHz, CDCl₃): δ = 153.9, 153.8, 149.6, 149.3 (4 signals from sp²-C in the aromatic ring), 151.7, 151.6, 147.6, 147.4, 146.6, 146.41, 146.40, 146.24, 146.23, 145.8, 145.7, 145.6, 145.444, 145.436, 145.37, 144.7, 144.5, 143.2, 142.60, 142.58, 142.09, 142.06, 142.0, 141.9, 141.7, 141.6, 140.290, 140.285, 136.0, 135.2 (30 signals from sp²-C in the C₆₀ core), 133.9, 124.0, 120.2, 117.9, 117.3, 117.1, 115.8, 115.7, 114.6, 113.9, 95.2, 94.1, 93.3, 88.8, 87.1, 83.0, 70.0, 69.7, 69.3, 69.2, 62.2 (CH in the C₆₀ core), 55.5 (quaternary sp³-C in the C₆₀ core), 31.97, 31.95, 31.94, 29.67, 29.67, 29.66, 29.63, 29.62, 29.47, 29.46, 29.45, 29.41, 29.394, 29.387, 26.3, 26.15, 26.069, 26.056, 22.763, 22.755, 22.724, 22.716, 14.24, 14.20, 14.15 ppm; FTIR (CH₂Cl₂ cast): $\tilde{\nu}$ = 2921, 2851, 1509 cm⁻¹; MALDI-TOF MS (dithranol as the matrix): *m/z*: calcd for C₃₀H₂₀O₁₂: 4787; found: 4788 [M]⁺.

Blank test reaction of [60]fullerene with LHMDs: A dark brownish slurry of pristine C₆₀ (45 mg, 0.063 mmol) in THF (30 mL) was ultrasonicated under N₂ for 4 h. LHMDs (0.31 mL, 0.31 mmol) was then added dropwise over 15 min and the mixture was kept stirring at room temperature for 2 h until a green color was observed. The reaction was quenched with TFA (0.1 mL) and the solvents were removed in vacuo. The resulted brownish solid was applied to a short silica plug and eluted with CS₂, affording the unreacted fullerene (41 mg, 0.057 mmol, 90% recovery). Afterwards, the silica plug was eluted with CS₂/CH₂Cl₂ (1:1) giving a brown solid (2 mg), which was characterized by ¹H NMR and MALDI-TOF MS as described in the text.

Electrochemistry: Cyclic voltammetry experiments were performed on a BAS-CV 50W instrument. A non-aqueous Ag/AgNO₃ electrode was used to serve as the reference electrode. A glass carbon electrode was used as the working electrode and a platinum wire as the counter-electrode. All experiments were conducted under a N₂ atmosphere using 3–5 mL solution containing 0.1 M Bu₄NBF₄ as the supporting electrolyte. The formal potential of 2 mM ferrocene in 0.1 M Bu₄NBF₄ and acetonitrile is 70 mV versus the Ag/AgNO₃ reference electrode.

Third-order NLO and TPA studies: The molecular third-order hyperpolarizabilities were measured by a differential optical Kerr effect (DOKE) setup as reported elsewhere.^[73] A multi-pass Ti:sapphire laser amplifier output 800 nm, 90 fs, 700 μJ pulses at a repetition rate of ~1 kHz. The beam was split into pump and probe beams, with the beamsplitter providing a 20:1 pump/probe energy ratio. The probe pulse was time-delayed with respect to the pump pulse by a computer controlled retro-reflector delay stage along the probe arm. The pump pulse is chopped by a 50% duty cycle chopper (CH) at 1/4 of the repetition rate (~270 Hz). Using a half-wave plate, the pump pulse was polarized 45° to the horizontal and was focused onto a 1 mm path-length quartz cuvette that was filled with a sample solution. The pump beam was directed to the sample and was nearly collinear (ca. 3°) with the circular-polarized probe beam. Attenuation control was present for both beams. At the sample, 0.05 μJ and 1–4 μJ pulses were typically used for the probe and pump beams respectively. The pump beam was blocked after the sample, while the probe beam was allowed to travel to a Wollaston polarizer acting as the analyzer. Here, the two transmitted beams were separated and directed to balanced photodiodes. Photodiode A received the horizontally polarized beam, and photodiode B received the vertically polarized beam. The sum and difference (A+B and A–B, respectively) of these signals were sent to separate lock-in amplifiers. The A–B signal was detected at the chopped frequency, and A+B was detected at the laser repetition rate frequency. Finally, these signals were sent to a data acquisition board enroute to a personal computer that is used for analysis and delay-stage control.

When the input pump polarization is aligned with one of the analyzer's axes (i.e., vertical or horizontal, in our case) the detected signal is proportional to the imaginary component of the nonlinearity, $\text{Im}(\gamma)$, and thus gives the nonlinear absorption response of the samples. On the other hand, when the input pump polarization is 45° to the analyzing directions, the detected signal is proportional to both the real and imaginary components of γ . Thus, by iterative scans with both polarizations, the real and imaginary components of the third-order optical nonlinearities are separated.^[73]

All samples were prepared as solutions in CH_2Cl_2 after a period of ultrasonication, and then transferred into 1.0 mm path-length quartz cuvettes for measurement.

Acknowledgements

This work was supported by the Welch Foundation of Texas, the Defense Advanced Research Projects Agency (DARPA), the Office of Naval Research and the Penn State MRSEC funded by the National Science Foundation (NSF). The NSF provided partial funding for the 400 (CHEM 0075728) and 500 MHz NMR (CHE-708978). We thank Dr. I. Chester of FAR Research Inc. for providing trimethylsilylacetylene. Y.Z. thanks the NSERC of Canada for providing a postdoctoral fellowship. A.D.S. thanks NSERC of Canada and the Alberta Ingenuity Fund for financial support.

- [1] R. Kiebooms, R. Menon, K. Lee in *Handbook of Advanced Electronic and Photonic Materials and Devices* (Ed.: H. S. Nalwa), Academic Press, San Diego, **2001**.
- [2] *Electronic Materials: The Oligomer Approach* (Eds.: K. Müllen, G. Wegner), Wiley-VCH, Weinheim, **1998**.
- [3] G. I. Stegeman in *Organic Materials for Non-Linear Optics, Vol. II* (Eds.: R. A. Hann, D. Bloor), RSC, Cambridge, **1991**, pp. 311–323.
- [4] R. E. Martin, F. Diederich, *Angew. Chem.* **1999**, *111*, 1440–1469; *Angew. Chem. Int. Ed.* **1999**, *38*, 1350–1377.
- [5] R. R. Tykwinski, Y. Zhao, *Synlett* **2002**, 1939–1953.
- [6] A. D. Slepokov, F. A. Hegmann, S. Eisler, E. Elliott, R. R. Tykwinski, *J. Chem. Phys.* **2004**, *120*, 6807–6810.
- [7] U. H. F. Bunz, *Chem. Rev.* **2000**, *100*, 1605–1644.
- [8] R. J. O. M. Hoofman, M. P. de Haas, L. D. A. Siebbeles, J. M. Warman, *Nature* **1998**, *392*, 54–56.
- [9] R. H. Friend, R. W. Gymer, A. B. Holmes, J. H. Burroughes, R. N. Marks, C. Taliani, D. D. C. Bradley, D. A. Dos Santos, J. L. Brédas, M. Lögdlund, W. R. Salaneck, *Nature* **1999**, *397*, 121–128.
- [10] *Polythiophenes: Electrically Conductive Polymers* (Eds.: G. Schopf, G. Kossmehl), Springer, New York, **1997**.
- [11] H. Sirringhaus, P. J. Brown, R. H. Friend, M. M. Nielsen, K. Bechgaard, B. M. W. Langeveld-Voss, A. J. H. Spiering, R. A. J. Janssen, E. W. Meijer, P. Herwig, D. M. de Leeuw, *Nature* **1999**, *401*, 685–688.
- [12] *Handbook of Oligo- and Polythiophenes* (Ed.: D. Fichou), Wiley-VCH, Weinheim, **1999**.
- [13] *Molecular Electronics-Science and Technology* (Ed.: A. Aviram), American Institute of Physics, New York, **1992**.
- [14] J. M. Tour, *Acc. Chem. Res.* **2000**, *33*, 791–804.
- [15] *Photonic and Optoelectronic Polymers* (Eds.: S. A. Jenekhe, K. J. Wynne), ACS, Washington, **1997**.
- [16] *Conjugated Polymeric Materials: Opportunities in Electronics, Optoelectronics and Molecular Electronics* (Eds.: J. L. Brédas, R. R. Chance), Kluwer Academic Publishers, Dordrecht, **1990**.
- [17] *Polymers for Second-Order Nonlinear Optics* (Eds.: G. A. Lindsay, K. D. Singer), ACS, Washington, DC, **1995**.
- [18] T. A. Skotheim, R. L. Elsenbaumer, J. R. Reynolds, *Handbook of Conducting Polymers*, Marcel Dekker, New York, **1998**.
- [19] *Organic, Metallo-Organic, and Polymeric Materials for Nonlinear Optical Applications* (Eds.: S. R. Marder, J. W. Perry), SPIE, Bellingham, **1994**.
- [20] *Buckminsterfullerenes* (Eds.: W. E. Billups, M. A. Ciufolini), VCH, New York, **1993**.
- [21] R. Taylor, *Lecture Notes on Fullerene Chemistry: A Handbook for Chemists*, Imperial College Press, London, **1999**.
- [22] D. M. Guldi, M. Prato, *Acc. Chem. Res.* **2000**, *33*, 695–730.
- [23] a) D. M. Guldi, P. V. Kamat in *Fullerenes: Chemistry, Physics, and Technology* (Eds.: K. M. Kadish, R. S. Ruott), Wiley, New York, **2000**, pp. 225–282; b) D. M. Guldi, N. Martín, *Fullerenes: From Synthesis to Optoelectronic Properties*, Kluwer Academic Publishers, Dordrecht, **2002**.
- [24] H. Imahori, *Org. Biomol. Chem.* **2004**, *2*, 1425–1433.
- [25] L. Sánchez, I. Pérez, N. Martín, D. M. Guldi, *Chem. Eur. J.* **2003**, *9*, 2457–2468.
- [26] D. González-Rodríguez, T. Torres, D. M. Guldi, J. Rivera, M. Á. Herranz, L. Echevoyen, *J. Am. Chem. Soc.* **2004**, *126*, 6301–6313.
- [27] A. Cravino, N. S. Sariciftci, *J. Mater. Chem.* **2002**, *12*, 1931–1943.
- [28] H. Yamada, H. Imahori, Y. Nishimura, I. Yamazaki, T. K. Ahn, S. K. Kim, D. Kim, S. Fukuzumi, *J. Am. Chem. Soc.* **2003**, *125*, 9129–9139.
- [29] D. Hirayama, K. Takimiya, Y. Aso, T. Otsubo, T. Hasobe, H. Yamada, H. Imahori, S. Fukuzumi, Y. Sakata, *J. Am. Chem. Soc.* **2002**, *124*, 532–533.
- [30] K. Ohkubo, H. Kotani, J. Shao, Z. Ou, K. M. Kadish, G. Li, R. K. Pandey, M. Fujitsuka, O. Ito, H. Imahori, S. Fukuzumi, *Angew. Chem.* **2004**, *116*, 871–871; *Angew. Chem. Int. Ed.* **2004**, *43*, 853–856.
- [31] M. Lamrani, R. Hamasaki, M. Mitsuishi, T. Miyashita, Y. Yamamoto, *Chem. Commun.* **2000**, 1595–1596.
- [32] E. Koudoumas, M. Konstantaki, A. Mavromanolakis, S. Couris, M. Fanti, F. Zerbetto, K. Kordatos, M. Prato, *Chem. Eur. J.* **2003**, *9*, 1529–1534.
- [33] Q. Chen, L. Kuang, E. H. Sargent, Z. Y. Wang, *Appl. Phys. Lett.* **2003**, *83*, 2115–2117.
- [34] M. Maggini, C. D. Faveri, G. Scorrano, M. Prato, G. Brusatin, M. Guglielmi, M. Meneghetti, R. Signorini, R. Bozio, *Chem. Eur. J.* **1999**, *5*, 2501–2510.
- [35] a) K. Tada, M. Onoda, *Adv. Funct. Mater.* **2004**, *14*, 139–144; b) N. S. Sariciftci, A. J. Heeger in *Handbook of Organic Conductive Molecules and Polymers, Vol. 1 Charge-Transfer Salts, Fullerenes and Photoconductors* (Ed: H. S. Nalwa), Wiley, **1997**, pp. 411–455.
- [36] M. Maggini, G. Scorrano, M. Prato, G. Brusatin, P. Innocenzi, M. Guglielmi, A. Renier, R. Signorini, M. Meneghetti, R. Bozio, *Adv. Mater.* **1995**, *7*, 404–406.
- [37] J. L. Atwood, L. J. Barbour, P. J. Nichols, C. L. Raston, C. A. Sandoval, *Chem. Eur. J.* **1999**, *5*, 990–996.
- [38] K. Komatsu, K. Fujiwara, Y. Murata, T. Braun, *J. Chem. Soc. Perkin Trans. 1* **1999**, 2963–2966.
- [39] Y. Liu, H. Wang, P. Liang, H.-Y. Zhang, *Angew. Chem.* **2004**, *116*, 2744–2748; *Angew. Chem. Int. Ed.* **2004**, *43*, 2690–2694.
- [40] S. R. Wilson, D. I. Schuster, B. Nuber, M. S. Meier, M. Maggini, N. Prato, R. Taylor in *Fullerene: Chemistry, Physics, and Technology* (Eds: K. M. Kadish, P. S. Ruott), Wiley, New York, pp. 91–176.
- [41] R. Taylor, *The chemistry of fullerenes*, World Scientific, Singapore, **1995**.
- [42] W. Fu, J.-K. Feng, G.-B. Pan, X. Zhang, *Theor. Chem. Acc.* **2001**, *106*, 241–250.
- [43] S. Zhang, L. Gan, C. Huang, M. Lu, J. Pan, X. He, *J. Org. Chem.* **2002**, *67*, 883–891.
- [44] A. I. de Lucas, N. Martín, L. Sánchez, C. Seoane, *Tetrahedron Lett.* **1996**, *37*, 9391–9394.
- [45] Y. Sun, T. Drovetskaya, R. D. Bolskar, R. Bau, P. D. W. Boyd, C. A. Reed, *J. Org. Chem.* **1997**, *62*, 3642–3649.
- [46] a) C. Atienza, B. Insuasty, C. Seoane, N. Martín, J. Ramey, G. M. A. Rahman, D. M. Guldi, *J. Mater. Chem.* **2005**, *15*, 124–132; b) J. L. Segura, E. M. Priego, N. Martín, C. Luo, D. M. Guldi, *Org. Lett.* **2000**, *2*, 4021–4024.
- [47] V. Mamane, O. Riant, *Tetrahedron* **2001**, *57*, 2555–2561.
- [48] S. Higashida, H. Imahori, T. Kaneda, Y. Sakata, *Chem. Lett.* **1998**, 605–606.

- [49] J.-F. Nierengarten, C. Schall, J.-F. Nicoud, *Angew. Chem.* **1998**, *110*, 2037–2040; *Angew. Chem. Int. Ed.* **1998**, *37*, 1934–1936.
- [50] N. Armaroli, C. Boudon, D. Felder, J.-P. Gisselbrecht, M. Gross, G. Marconi, J.-F. Nicoud, J.-F. Nierengarten, V. Vivinelli, *Angew. Chem.* **1999**, *111*, 3895–3899; *Angew. Chem. Int. Ed.* **1999**, *38*, 3730–3733.
- [51] G. Susana, N. Martín, D. M. Guldi, *J. Org. Chem.* **2003**, *68*, 779–791.
- [52] M. Diekers, C. Luo, D. M. Guldi, A. Hirsch, *Chem. Eur. J.* **2002**, *8*, 979–991.
- [53] R. Kessinger, C. Thilgen, T. Mordasini, F. Diederich, *Helv. Chim. Acta* **2000**, *83*, 3069–3096.
- [54] J. Knol, J. C. Hummelen, *J. Am. Chem. Soc.* **2000**, *122*, 3226–3227.
- [55] J.-F. Nierengarten, A. Herrmann, R. R. Tykwinski, M. Rüttimann, F. Diederich, *Helv. Chim. Acta* **1997**, *80*, 293–316.
- [56] G. P. Miller, J. Briggs, J. Mack, P. A. Lord, M. M. Olmstead, A. Balch, *Org. Lett.* **2003**, *5*, 4199–4202.
- [57] G. P. Miller, J. Briggs, *Org. Lett.* **2003**, *5*, 4203–4206.
- [58] a) T. Gu, J.-F. Nierengarten, *Tetrahedron Lett.* **2001**, *42*, 3175–3178; b) J.-F. Nierengarten, T. Gu, G. Hadziioannou, D. Tsamouras, V. Krasnikov, *Helv. Chim. Acta* **2004**, *87*, 2948–2966.
- [59] D. M. Guldi, C. Luo, A. Swartz, *J. Org. Chem.* **2002**, *67*, 1141–1152.
- [60] P. A. van Hal, J. Knol, B. M. W. Langeveld-Voss, S. C. J. Meskers, J. C. Hummelen, R. A. J. Janssen, *J. Phys. Chem. A* **2000**, *104*, 5974–5988.
- [61] Y. Obara, K. Takimiya, Y. Aso, T. Otsubo, *Tetrahedron Lett.* **2001**, *42*, 6877–6881.
- [62] J. Ikemoto, K. Takimiya, Y. Aso, T. Otsubo, M. Fujitsuka, M. Ito, *Org. Lett.* **2002**, *4*, 309–311.
- [63] J.-F. Eckert, J.-F. Nicoud, J.-F. Nierengarten, S.-G. Liu, L. Echegoyen, F. Barigelletti, N. Armaroli, L. Ouali, V. Krasnikov, G. Hadziioannou, *J. Am. Chem. Soc.* **2000**, *122*, 7467–7479.
- [64] E. Peeters, P. A. van Hal, J. Knol, C. J. Brabec, N. S. Sariciftci, J. C. Hummelen, R. A. J. Janssen, *J. Phys. Chem. B* **2000**, *104*, 10174–10190.
- [65] S.-G. Liu, C. Martineau, J.-M. Raimundo, J. Roncali, L. Echegoyen, *Chem. Commun.* **2001**, 913–914.
- [66] P. Timmerman, L. E. Witschel, F. Diederich, *Helv. Chim. Acta* **1996**, *79*, 6–20.
- [67] K. Komatsu, N. Takimoto, Y. Murata, T. S. M. Wan, T. Wang, *Tetrahedron Lett.* **1996**, *37*, 6153–6156.
- [68] T. Tanaka, K. Komatsu, *J. Chem. Soc. Perkin Trans. 1* **1999**, 1671–1675.
- [69] F. Wudl, T. Sukuki, M. Prato, *Synth. Met.* **1993**, *59*, 297–305.
- [70] R. Hamasaki, M. Ito, M. Lamrani, M. Mitsuishi, T. Miyashita, Y. Yamamoto, *J. Mater. Chem.* **2003**, *13*, 21–26.
- [71] B. Knight, N. Martín, T. Ohno, E. Ortí, C. Rovira, J. Veciana, J. Vidal-Gancedo, P. Viruela, R. Viruela, F. Wudl, *J. Am. Chem. Soc.* **1997**, *119*, 9871–9882.
- [72] Y. Shirai, Y. Zhao, L. Cheng, J. M. Tour, *Org. Lett.* **2004**, *6*, 2129–2132.
- [73] A. D. Slepikov, F. A. Hegmann, Y. Zhao, R. R. Tykwinski, K. Kamada, *J. Chem. Phys.* **2002**, *116*, 3834–3840.
- [74] K. Komatsu, Y. Murata, N. Takimoto, S. Mori, N. Sugita, T. S. M. Wan, *J. Org. Chem.* **1994**, *59*, 6101–6102.
- [75] K. Fujiwara, Y. Murata, T. S. M. Wan, K. Komatsu, *Tetrahedron* **1998**, *54*, 2049–2058.
- [76] S. M. Draper, M. Delamesiere, E. Champeil, B. Twamley, J. J. Byrne, C. Long, *J. Organomet. Chem.* **1999**, *589*, 157–167.
- [77] Y. Murata, M. Ito, K. Komatsu, *J. Mater. Chem.* **2002**, *12*, 2009–2020.
- [78] See, for example: a) C. A. Breen, T. Deng, T. Breiner, E. L. Thomas, T. M. Swager, *J. Am. Chem. Soc.* **2003**, *125*, 9942–9943; b) D. A. M. Egbe, C. Bader, E. Klemm, L. Ding, F. E. Karasz, U.-W. Grummt, E. Birckner, *Macromolecules* **2003**, *36*, 9303–9312; c) D. A. M. Egbe, B. Cornelia, J. Nowotny, W. Günther, E. Klemm, *Macromolecules* **2003**, *36*, 5459–5469; d) Q. Chu, Y. Pang, L. Ding, F. E. Karasz, *Macromolecules* **2003**, *36*, 3848–3853; e) C.-Z. Zhou, T. Liu, J.-M. Xu, Z.-K. Chen, *Macromolecules* **2003**, *36*, 1457–1464; f) J. Chen, H. Liu, W. A. Weimer, M. D. Halls, D. H. Waldeck, G. C. Walker, *J. Am. Chem. Soc.* **2002**, *124*, 9034–9035; g) D. A. M. Egbe, H. Tillmann, E. Birckner, E. Klemm, *Macromol. Chem. Phys.* **2001**, *202*, 2712–2726; h) G. Giardina, P. Rosi, A. Ricci, C. L. Sterzo, *J. Polym. Sci. Polym. Chem. Ed.* **2000**, *38*, 2603–2621; i) A. Khatyr, R. Ziessel, *J. Org. Chem.* **2000**, *65*, 3126–3134; j) L. Kloppenburg, D. Jones, U. H. F. Bunz, *Macromolecules* **1999**, *32*, 4194–4203; k) T. M. Swager, C. J. Gil, M. S. Wrighton, *J. Phys. Chem.* **1995**, *99*, 4886–4893; l) M. Moroni, J. Le Moigne, S. Luzzati, *Macromolecules* **1994**, *27*, 562–571; m) and references cited in these papers to other relevant papers; n) P. J. Fagan, P. J. Krusic, D. H. Evans, S. A. Lerke, E. Johnston, *J. Am. Chem. Soc.* **1992**, *114*, 9697–9699; o) W. W. Win, M. Kao, M. Eiermann, J. J. McNamara, F. Wudl, D. L. Pole, K. Kassam, J. Warkentin, *J. Org. Chem.* **1994**, *59*, 5871–5876; p) S. Huang, J. M. Tour, *Tetrahedron Lett.* **1999**, *40*, 3347–3350.
- [79] G. I. Stegeman, A. Miller in *Photonics in Switching, Vol. I* (Ed.: J. E. Midwinter), Academic Press, San Diego, **1993**.
- [80] J. E. Ehrlich, X. L. Wu, Y. L. Lee, Z. Y. Hu, H. Rockel, S. R. Marder, J. W. Perry, *Opt. Lett.* **1997**, *22*, 1843–1845.
- [81] A. A. Said, C. Wamsley, D. J. Hagan, E. W. van Stryland, B. A. Reinhardt, P. Roderer, A. G. Dillard, *Chem. Phys. Lett.* **1994**, *228*, 646–650.
- [82] G. S. He, C. F. Zhao, J. D. Bhawalkar, P. N. Prasad, *Appl. Phys. Lett.* **1995**, *67*, 3703–3705.
- [83] W. Denk, J. H. Strickler, W. W. Webb, *Science* **1990**, *248*, 73–76.
- [84] D. A. Parthenopoulos, P. M. Rentzepis, *Science* **1989**, *245*, 843–845.
- [85] J. H. Strickler, W. W. Webb, *Opt. Lett.* **1991**, *16*, 1780–1782.
- [86] B. H. Cumpston, S. P. Ananthavel, S. Barlow, D. L. Dyer, J. E. Ehrlich, L. L. Erskine, A. A. Heikal, S. M. Kuebler, I.-Y. S. Lee, D. McCord-Maughon, J. Qin, H. Rockel, M. Rumi, X.-L. Wu, S. R. Marder, J. W. Perry, *Nature* **1999**, *389*, 51–54.
- [87] W. H. Zhou, S. M. Kuebler, K. L. Braun, T. Y. Yu, J. K. Cammack, C. K. Ober, J. W. Perry, S. R. Marder, *Science* **2002**, *296*, 1106–1109.
- [88] S. Kawata, H.-B. Sun, T. Tanaka, K. Tanaka, *Nature* **2001**, *412*, 697–698.
- [89] H. Stiel, K. Teuchner, A. Paul, W. Freyer, D. J. Leupold, *J. Photochem. Photobiol. A* **1994**, *80*, 289–298.
- [90] R. L. Sutherland, D. G. McLean, S. Kirkpatrick, *Handbook of Non-linear Optics*, Marcel Dekker, New York, **2003**.
- [91] S. Kershaw in *Characterization Techniques and Tabulations for Organic Nonlinear Optical Materials* (Eds.: M. G. Kuzyk, C. W. Dirk), Marcel Dekker, New York, **1998**.
- [92] W. J. Blau, H. J. Byrne, D. J. Cardin, T. J. Dennis, J. P. Hare, H. W. Kroto, R. Taylor, D. R. M. Walton, *Phys. Rev. Lett.* **1991**, *67*, 1423–1425.
- [93] M. F. Yung, K. Y. Wong, *Appl. Phys. B* **1998**, *66*, 585–588.
- [94] J. Li, S. Wang, H. Yang, Q. Gong, X. An, H. Chen, D. Qiang, *Chem. Phys. Lett.* **1998**, *288*, 175–178.
- [95] L. Geng, J. C. Wright, *Phys. Rev. Lett.* **1996**, *76*, 105–111.
- [96] S. J. A. van Gisbergen, J. G. Snijders, E. J. Baerends, *Phys. Rev. Lett.* **1997**, *78*, 3097–3100.
- [97] L. Y. Chiang, P. A. Padmawar, T. Canteenwala, L.-S. Tan, G. S. He, R. Kannan, R. Vaia, T.-C. Lin, Q. Zheng, P. N. Prasad, *Chem. Commun.* **2002**, 1854–1855.
- [98] S. Wang, W. Huang, R. Liang, Q. Gong, H. Li, H. Chen, D. Qiang, *Phys. Rev. B* **2001**, *63*, 153408.
- [99] B. L. Yu, H. P. Xia, C. S. Zhu, F. X. Gan, *Appl. Phys. Lett.* **2002**, *81*, 2701–2703.
- [100] C.-K. Wang, P. Macak, Y. Luo, H. Agren, *J. Chem. Phys.* **2001**, *114*, 9813–9820.
- [101] A. Abbotto, L. Beverina, R. Bozio, S. Bradamante, C. Ferrante, G. A. Pagani, R. Signorini, *Adv. Mater.* **2000**, *12*, 1963.
- [102] M. Albota, D. Beljonne, J. L. Brédas, J. E. Ehrlich, J.-Y. Fu, A. A. Heikal, S. E. Hess, T. Kogej, M. D. Levin, S. R. Marder, D. McCord-Maughon, J. W. Perry, H. Röckel, M. Rumi, G. Subramaniam, W. W. Webb, X.-L. Wu, C. Xu, *Science* **1998**, *281*, 1653–1656.

- [103] B. A. Reinhardt, L. L. Brott, S. J. Clarkson, A. G. Dillard, J. C. Bhatt, R. Kannan, L. Yuan, G. S. He, P. N. Prasad, *Chem. Mater.* **1998**, *10*, 1863–1874.
- [104] M. Barzoukas, M. Blanchard-Desce, *J. Chem. Phys.* **2000**, *113*, 3951–3959.
- [105] E. Zojer, D. Beljonne, P. Pacher, J.-L. Brédas, *Chem. Eur. J.* **2004**, *10*, 2668–2680.
- [106] M. Rumi, J. E. Ehrlich, A. A. Heikal, J. W. Perry, S. Barlow, Z. Hu, D. McCord-Maughon, T. C. Parker, H. Röckel, S. Thayumanavan, S. R. Marder, D. Beljonne, J.-L. Brédas, *J. Am. Chem. Soc.* **2000**, *122*, 9500–9510.
- [107] D. Beljonne, W. Wenseleers, E. Zojer, Z. Shuai, H. Vogel, S. J. K. Pond, J. W. Perry, S. R. Marder, J.-L. Brédas, *Adv. Funct. Mater.* **2002**, *12*, 631–641.
- [108] W.-H. Lee, H. Lee, J.-A. Kim, J.-H. Choi, M. Cho, S.-J. Jeon, B. R. Cho, *J. Am. Chem. Soc.* **2001**, *123*, 10658–10667.
- [109] M. Drobizhev, A. Karotki, A. Rebane, C. W. Spangler, *Opt. Lett.* **2001**, *26*, 1081–1083.
- [110] B. R. Cho, M. J. Piao, K. H. Son, S. H. Lee, S. J. Yoon, S.-J. Jeon, M. Cho, *Chem. Eur. J.* **2002**, *8*, 3907–3916.
- [111] R. Lascola, J. C. Wright, *Chem. Phys. Lett.* **1997**, *269*, 79–84.
- [112] In a 2 mm solution of **31** in CH₂Cl₂, some undissolved residue was observed. The quantity of this particulate was extremely small and should not impact the concentration. If, however, the concentration were lower than reported, the molecular nonlinearities reported herein for **31** would only be greater than reported.
- [113] K. Kamada, K. Ohta, Y. Iwase, K. Kondo, *Chem. Phys. Lett.* **2003**, *372*, 386–393.
- [114] Nonlinear absorption measurements conducted with ns pulses often show signals that are orders of magnitude higher than those conducted with fs pulses. This is mainly due to signals from excited-state absorption mixing with pure TPA signals. However, comparisons of the same “AFX” compounds’ TPA cross-sections have been done by the same group at both pulse duration regimes. We have also studied an “AFX” compound (not discussed herein) that allows for scaling of our fs results for comparisons with ns results. See: ref. [82] and [97].
- [115] H. S. Nalwa in *Nonlinear Optics for Organic Molecules and Polymers* (Eds.: H. S. Nalwa, S. o. Miyata), CRC Press, New York, **1997**, pp. 571–609.
- [116] A. Willetts, J. E. Rice, D. M. Burland, *J. Chem. Phys.* **1992**, *97*, 7590–7595.
- [117] D. M. Guldi, G. Torres-Garcia, J. Mattay, *J. Phys. Chem. A* **1998**, *102*, 9679–9685.
- [118] S.-J. Chung, K.-S. Kim, T.-C. Lin, G. S. He, J. Swiatkiewicz, P. N. Prasad, *J. Phys. Chem. B* **1999**, *103*, 10741–10745.
- [119] G. S. He, J. Swiatkiewicz, Y. Jing, P. N. Prasad, B. A. Reinhardt, L.-S. Tan, R. Kannan, *J. Phys. Chem. A* **2000**, *104*, 4805–4810.
- [120] S. Polyakov, F. Yoshino, M. Liu, G. Stegeman, *Phys. Rev. B* **2004**, *69*, 115421.
- [121] L. D. Ziegler, X. J. Jordanides, *Chem. Phys. Lett.* **2002**, *352*, 270–280.
- [122] Q. Zhou, P. J. Carroll, T. M. Swager, *J. Org. Chem.* **1994**, *59*, 1294–1301.

Received: November 23, 2004

Published online: April 7, 2005